DECADAL SCALE VEGETATION MAPS FOR THE BOREAL FOREST SURROUNDING FAIRBANKS, ALASKA

By

Hannah E Huhman, B.S.

A Thesis Submitted in Partial Fulfillment of the Requirements

for the Degree of

Master of Science

in

Geosciences: Remote Sensing

University of Alaska Fairbanks

August 2018

APPROVED:

Anupma Prakash, Committee Chair

Jordi Cristóbal Rosselló, Committee Member

Jon Dewitz, Committee Member

Paul McCarthy, Chair

Department of Geosciences

Leah Berman, Interim Dean

College of Natural Science and Mathematics

Michael Castellini, *Dean of the Graduate School*

Abstract

Vegetation maps of a selected area within the boreal forest surrounding Fairbanks, Alaska, have been generated for the nominal years of 1985, 1995, 2005, and 2015 using Landsat 4 and 5 Thematic Mapper and Landsat 8 Operational Land Imager surface reflectance products at 30 meter spatial resolution using a decision tree classification. The maps include 9 U.S. Geological Survey (USGS) vegetation classes, as well as barren land, open water, and ice/snow classes that are consistent with the classes identified in the 2001 National Land Cover Database (NLCD) map of Alaska generated by the USGS. Classification steps are based on USGS methodology, with refinements for the boreal forest, to ensure further comparison to the 2001 USGS NLCD map for Alaska. The overall weighted accuracies of first order estimates of data quality using cross validation are 93.2%, 88.4%, 93.3%, and 86.9% for the nominal years of 1985, 1995, 2005, and 2015 maps, respectively, compared to 81.8% accuracy for the USGS NLCD 2001 product. This study demonstrates that the spatial and spectral resolution of Landsat data is the best available for mapping the vegetation of Alaska's boreal forest at 1:50,000 scale. It also shows that the boreal forests surrounding Fairbanks, Alaska have witnessed a decrease in the growth of evergreen forests, an expansion of shrub and an increase in wetland distribution, all of which have been reported as impacts of a warming climate in the Arctic and Sub-arctic.

Table of Contents

Page

Title Page i

Abstract iii

List of Figures ix

List of Tables xi

List of Equations xiii

Acknowledgements xiii

1. INTRODUCTION 1

1.1 Changes to the Boreal Forest and Their Implications 1

1.2 Vegetation Maps of the Alaskan Boreal Forest 3

1.3 Study Goal 5

1.4 Study Area 6

1.4.1 Interior Alaska 6

1.4.2 Study Area Description 7

1.4.3 Vegetation Classes 8

2. DATA 15

2.1 Remote Sensing and Ancillary Data **15**

2.2 Field Data **19**

3. METHODS **23**

3.1 Pre-processing **24**

3.2 Classification Process **27**

3.3 Post-processing **29**

4. RESULTS **31**

4.1 Vegetation Classification Maps **31**

4.1.1 1985 Vegetation Classification Map *31*

4.1.2 1995 Vegetation Classification Map *33*

4.1.3 2005 Vegetation Classification Map *35*

4.1.4 2015 Vegetation Classification Map 37

4.2 Classification Model Performance **39**

4.2.1 1985 Classification Model Performance *41*

4.2.2 1995 Classification Model Performance *43*

4.2.3 2005 Classification Model Performance *45*

4.2.4 2015 Classification Model Performance *47*

4.3 Vegetation Classification Map Overall Weighted Accuracy **48**

4.4 Distribution of Vegetation by Class **49**

4.5 Vegetation Cross-tabulation **52**

5. DISCUSSION **57**

5.1 Limitations in Using Multitemporal Datasets for Vegetation Classification **57**

5.2 Classification Model Evaluation by Vegetation Class **59**

5.3 Cross-tabulated Area Analysis **63**

5.4 Comparative Analysis of Vegetation Classification Maps **63**

6. CONCLUSION AND FUTURE IMPROVEMENTS **67**

References 70

List of Figures

		Page
1	Study area location map	7
2	Example of a deciduous forest	9
3	Examples of evergreen forests	9
4	Example of a mixed forest	10
5	Example of a dwarf shrub dominated area	10
6	Examples of shrubland	11
7	Example of a sedge dominated landscape	11
8	Example of grassland	12
9	Example of a woody wetland	12
10	Example of emergent herbaceous wetlands	13
11	Example of barren land	13
12	Landsat scene locations	18
13	Landsat scene overlap	19
14	Distribution of all available field data shown in red	21
15	Methodology flow chart	23
16	False natural and false color composite comparison	24
17	Vegetation disturbances for Alaska	25
18	1985 Vegetation Map	32

19 1995 Vegetation Map 34

20 2005 Vegetation Map 36

21 2015 Vegetation Map 38

22 Vegetation class distribution for 1985..... 50

23 Vegetation class distribution for 1995..... 50

24 Vegetation class distribution for 2005..... 51

25 Vegetation class distribution for 2015..... 51

List of Tables

Page

1 Vegetation Classes 8

2 Landsat 4-5 TM and Landsat 8 OLI spectral and spatial resolution 16

3 Landsat scene specifications 17

4 1985 map northwest and southwest scenes classification model performance in number of pixels 41

5 1985 map northeast and southeast scenes classification model performance in number of pixels 41

6 1995 map northwest and southwest scenes classification model performance in number of pixels 43

7 1995 map northeast and southeast scenes classification model performance in number of pixels 43

8 2005 map northwest scene classification model performance in number of pixels 45

9 2005 map northeast and southeast scenes classification model performance in number of pixels 45

10 2005 map southwest scene classification model performance in number of pixels 46

11 2015 northwest and southwest scenes classification model performance in number of pixels 47

12 2015 map northeast and southeast scenes classification model performance in number of pixels 47

13 Overall weighted accuracy for 1985 vegetation map 48

14 Overall weighted accuracy for 1995 vegetation map 48

15 Overall weighted accuracy for 2005 vegetation map 49

16 Overall weighted accuracy for 2015 vegetation map 49

17 Cross-tabulation between 1985-1995 vegetation maps in percent area 52

18 Cross-tabulation between 1995-2005 vegetation maps in percent area 53

19 Cross-tabulation between 2005-2015 vegetation maps percent area 53

20 Cross-tabulation between 1985-2015 vegetation maps in percent area 54

21 Cross-tabulation between 1995-2015 vegetation maps in percent area 54

22 Cross-tabulation in percent area between the southeast and southwest corners of the 1985-2015 vegetation maps 55

23 Cross-tabulation percent area between 1985-2015 vegetation maps, with fire scars masked 55

24 Cross-tabulation in percent area between 1995-2015 vegetation maps, with fire scars masked 55

List of Equations

Page

1 The potential information generated by dividing training classes, T, into subsets n..... 27

2 The gain ratio conveys the useful information for the classification generated by the split..... 27

3 The KHATT statistic 40

Acknowledgements

This research is made possible through the support from Alaska EPSCoR NSF award #OIA-1208927 and the state of Alaska, as well as the College of Natural Science and Mathematics at the University of Alaska Fairbanks. Thank you to the U.S. Geological Survey and Hexagon Geospatial for providing me with the necessary software. Thank you to Jamie Hollingsworth and the Bonanza Creek Long Term Ecological Research Network (NSF Award DEB-1636476, USDA Forest Service, Pacific northwest Research Station RJVA-PNW-01-JV-11261952-231) for providing me with their ground truth data. Thank you to Kirk Hogensen at the Alaska Satellite Facility for providing me with a Digital Elevation Model of my study area. Landsat Surface Reflectance products courtesy of the U.S. Geological Survey Earth Resources Observation and Science Center, Sioux Falls, South Dakota

1. INTRODUCTION

1.1. Changes to the Boreal Forest and Their Implications

Surface air temperatures in the Arctic have shown a significant increase especially in the past few decades (Serreze and Barry, 2011). Arctic amplification, referring to more rapid increases in air temperatures in the Arctic compared to other parts of the globe, is causing widespread melting of snow and ice, sea-ice retreat and a rise in the global sea level (Arctic Council, 2013; Serreze and Barry, 2011). Reconstructions from proxy sources indicate that Arctic air temperatures in the 20th century were the highest in the last 400 years (Serreze et al., 2000), and paleoclimate analysis indicates that the warming of the 20th century is likely to have been the largest of any century within the last 1000 years (Follan et al., 2001). Over the past 50 years, the Arctic has seen warming approximately twice that of the global rate (Walsh 2014), with an increase in air temperature of 0.35°C per decade since 1970 (McGuire et al., 2009). This shift in the climate is known as climate change, and it acts as a disturbance to the boreal forest; evidence has already been found that climate change has affected the Alaskan boreal forest in the following ways: a decrease in the health and growth of white spruce trees, an increase in insect infestation on both the landscape and regional scale, and an increase in both the number of severe burning forest fires, and the amount of area burned by these fires (Soja et al., 2007).

The boreal forest covers a large portion of the Earth, approximately 22% of the land surface, and is susceptible to a variety of disturbances, such as climate change, forest fires, insect infestation, and human interference (Chapin et al., 2000; Ott et al., 2006). Over at least the past three decades, Arctic and boreal ecosystems in Alaska and Western Canada have shown evidence of "greening" (Jia et al., 2003, Xu et al., 2013), with about a 14% increase in peak vegetation (Bhatt et al., 2010). In particular, the expansion of the distribution of deciduous shrubs is contributing to the greening trend (Heskel et al., 2013; Myers-Smith et al., 2011; Sturm et al., 2001), and is related to warmer temperatures. In contrast, some areas of the boreal forest are "browning" from greater coniferous tree mortality due to warmer temperatures and drier conditions (Goetz et al., 2005; Beck et al., 2011; Verbyla, 2008). With greater frequency and intensity of wildfires,

the boreal forest is shifting to more deciduous tree and shrub cover due to their higher drought tolerance and their ability to establish quickly after disturbance (Viereck, 1979; Suarez et al., 1999; Lloyd, 2005; Xu et al., 2013). Further, the northern boundary of the forest-tundra transition zone is expanding, both in latitude and elevation, tree heights are increasing, and shrubs are becoming denser and taller (Tape et al., 2006; Myers-Smith et al., 2011).

Wildfire, the primary disturbance in the boreal forest, is driven by climate change and has several implications on the surrounding ecosystems and humans that depend on the forest. Forest fires have been increasing in frequency and extent in the North American boreal forests; since the 1960s the frequency of large fire years increased from an average of 5 times per decade to 7 times per decade in the 1980s and 8 times per decade in the 1990s, and the extent of the burned area doubled (Kasischke and Turetsky, 2006). Black spruce (*Picea mariana*), a coniferous species that serves as a good fuel source, is currently the most widespread forest type in the interior of Alaska (Johnstone et al., 2010b). Vegetation regrowth patterns after intense fire in interior Alaska show that severely burning forest fires promote the deciduous tree species (e.g. Johnstone et al., 2010a). If the pattern of more frequent fires continues, Alaska is predicted to have more deciduous dominated forests in the future (Beck et al., 2011). This successional transition from coniferous dominated forests to deciduous dominated forests would be a change in fuel type, as deciduous vegetation is less flammable, and this could ultimately alter the fire regime and the resilience of the forest (Johnstone et al., 2010b). Depending on the scale of change, this transition would also affect local and regional changes such as habitat availability for subsistence flora and fauna, hydrology (evapotranspiration), and permafrost distribution (Johnstone et al., 2010b; Beck et al., 2011).

Successional changes to the climate also follow forest fires. The boreal region is a carbon sink, containing more than 30% of all terrestrial carbon. When forest fires burn, they release the large amounts of carbon they store as greenhouse gases directly into the atmosphere, which have lasting effects on the climate (Kasischke and Stocks, 2012). The loss of vegetation after fires affect exchanges between the atmosphere and heat, water, and gases, which ultimately affect

weather and climate. Smoke particles from fires interact directly with the scattering and absorption of atmospheric radiation, and can lead to changes in local cloud properties, air temperature, wind, and humidity (Liu et al., 2014). When forest fire smoke acts as Arctic air pollution, it reduces sea ice and snow albedo, which may be a contributing factor to thinning Arctic sea ice and glacial melting (Kim et al., 2005). The boreal forest is likely facing many changes, and these changes may have several serious implications, and need to be monitored.

1.2. Vegetation Maps of the Alaskan Boreal Forest

For changes to be recognized there needs to be a clear record of what the boreal forest has looked like in the past. There are only three land cover or vegetation map sources that cover the entirety of Alaska. These include the Vegetation Map and Classification: Northern, Western, and Interior Alaska (Boggs et al., 2012), the LANDFIRE Existing Vegetation Type (EVT) map (LANDFIRE 2012a), and the USGS National Land Cover Database (NLCD) (Homer et al., 2004), which have all had at least one update in recent years. Both the LANDFIRE EVT and the NLCD maps were generated in 2001, with the Vegetation Map and Classification: Northern, Western, and Interior Alaska generated in 2012. This means there is no statewide record of what the boreal forest in Alaska was like before 2001. Other than these state-wide maps, there are only smaller regional maps, such as the one from 2001 provided by Ustin and Xiao. This is little coverage compared to the rest of the conterminous United States. For example, the USGS has produced NLCD maps for the conterminous United States for the years of 1992, 2001, 2006, and 2011, but only have maps for Alaska for 2001 and 2011. Additionally, there are only 18 regional maps covering areas in Alaska suitable enough for the standards for the Vegetation Map and Classification: Northern, Western, and Interior Alaska (including the USGS NLCD and LANDFIRE EVT maps). Many of these regional maps are not available to the public as they are held within government agencies.

The Vegetation Map and Classification: Northern, Western, and Interior Alaska map was created by combining several regional maps developed over the last 31 years. Eighteen of the most current regional maps derived from either satellite imagery or aerial photos were converted to

raster datasets, resampled to 30 m pixel size, and mosaicked together. The classification legend consists of a two-tiered system; coarse scale classes are analogous to level III of the Alaska Vegetation Classification and contain 27 classes, and the fine scale classes are analogous to level IV of the Alaska Vegetation Classification and contain 374 classes (Viereck et al., 1992). The robust legend of this map makes it possible to study rarer vegetation habitats, the distribution of different plant communities, and to gain more detailed site descriptions for future studies (Boggs et al., 2012). Unfortunately, this vegetation map does not allow for change detection analysis as it was developed combining data from the last 31 years.

The LADFIRE EVT was generated with Landsat Thematic Mapper (TM) satellite imagery at 30 m spatial resolution, ground truth data from their LANDFIRE Public Reference Database (LPRD), various ancillary data such as DEM, slope, aspect, as well as biophysical gradient variables such as potential evapotranspiration, relative humidity, and soil water potential. A second set of biophysical gradients was used as well. This second set was a potential vegetation type map, which ensured the mapped vegetation types were constrained to geographic areas that were ecologically possible. A decision tree (DT) mapping algorithm, in this case See5 (https://www.rulequest.com/see5-info.html), was trained with three different dates of Landsat images for each path and row which was used to ensure the vegetation dynamic of the growing season was captured, ground truth data, and two biophysical ancillary datasets to map the existing vegetation type. The classification legend for the EVT product is a combination of ecological systems (or aggregated ecological systems) described by Comer at al., 2003, and the US National Vegetation Classification described by Grossman et al., 1998. The legend for EVT is not quite as robust as the legend for the Vegetation Map and Classification: Northern, Western, and Interior Alaska map, but more in depth than the legend for the USGS NLCD maps. The EVT map was specifically designed to provide data and support for landscape level management planning for forest fires, not for change detection analysis (Rollins, 2009; Zhu et al. 2006).

The USGS NLCD 2001 product was developed using a combination of Landsat 5 TM and Landsat 7 Enhanced Thematic Mapper plus (ETM+) at 30 m spatial resolution. Reference data used were

a combination of aerial photos and field data with information gained from partnering with other Federal programs, such as the United States Forest Service's Forest Inventory Analysis program. DEM, slope, and aspect, and in some cases regionally available information such as wetland and soil inventory were added. Ancillary data, such as population density, buffered roads, and NOAA City lights were used for the urban areas. Like the LANDFIRE EVT product, three Landsat scenes per path and row, plus the ancillary data were used to train the DT algorithm in C5 developed by RuleQuest, the linux base classification software of See5. The classification legend is the broadest of the three statewide maps discussed here. It consists of 16 classes and was modified from the Anderson Land Cover Classification System (Anderson, 1976). The objective of the USGS NLCD project was to provide consistent landcover information at a national scale, which allows for change detection analysis. Although the legend may not be as in depth as the previously mentioned products, often the in-depth classification schemes become too narrow to be utilized for a wide range of applications. Keeping the classes more broad means the products can be used for projects ranging from national to regional scales (Homer et al., 2004).

1.3. Study Goal

The goal of this study is to increase the temporal resolution of mapped vegetation for a selected part of interior Alaska by generating vegetation maps for the nominal years of 1985, 1995, 2005, and 2015 that are comparable to the USGS NLCD products. To insure compatibility, Landsat products at 30 m spatial resolution and 9 vegetation classes (defined in section 1.4.3) from the USGS NLCD legend were used. The same classification methodology as the USGS NLCD 2001 product (Homer et al., 2004) was refined for the study area. The products generated in this study are referred to as vegetation maps (as opposed to the USGS land cover products) because the majority of the land in the study area is covered by vegetation, and other categories such as urban, pasture, and cultivated crop areas were not classified.

1.4. Study Area

1.4.1. Interior Alaska

The study area (Figure 1) is located in the boreal forest surrounding the Fairbanks area in Interior Alaska. Interior Alaska is characterized as the intermontane plateau bound by the Brooks Range to the north, and the Alaska Range to the south. Throughout the plateau are smaller isolated mountain ranges, areas of gently sloping uplands, meandering braided rivers with expansive floodplains, and extensive flat lowland plains populated with thaw lakes (Johnstone et al., 2010b; van Cleve et al., 1983). In the lowlands of this region one can find large amounts of sand and gravel glacial outwash, carried by the Tanana River from glaciation in the Alaska Range. This glacial outwash has now been covered with finer alluvial sand and silt which have resulted in sandy soils near the main streams and silty soils further away from the streams. The uplands in this region are formed from a Precambrain formation of folded and jointed quartz-mica and quartzite schist, also known as Birch Creek schist. The uplands have been covered with micaceous loess originating from these glacial outwash plains of the Tanana River. The soils from the loess have migrated down ridges and come to rest on foot slopes or in narrow drainage ways. Soils on south facing slopes receive more heat and are generally better drained than soils on north facing slopes (Rieger et al., 1963). Soils throughout interior Alaska are relatively stunted in their morphological development, resulting in only three percent of the soils to have extensive profile development such as mollisols and spododols. Inceptisols, entisols and histols make up the other approximately 78%, 12%, and 7% respectively of the area (Rieger et al., 1963; van Cleve et al., 1983). Continuous and discontinuous permafrost varies throughout the region (Ustin and Xiao, 2001). The climate in Interior Alaska is continental, characterized by extremely cold winters with temperatures dropping to -50 °C in January, and warm dry summers with temperatures climbing to +33 degrees °C in July. There are drastic fluctuations in day length, with almost 22 hours on June 21st and less than 4 hours on December 21st. The short growing season is only 135 days, from May to mid-September (Hinzman et al., 2006).

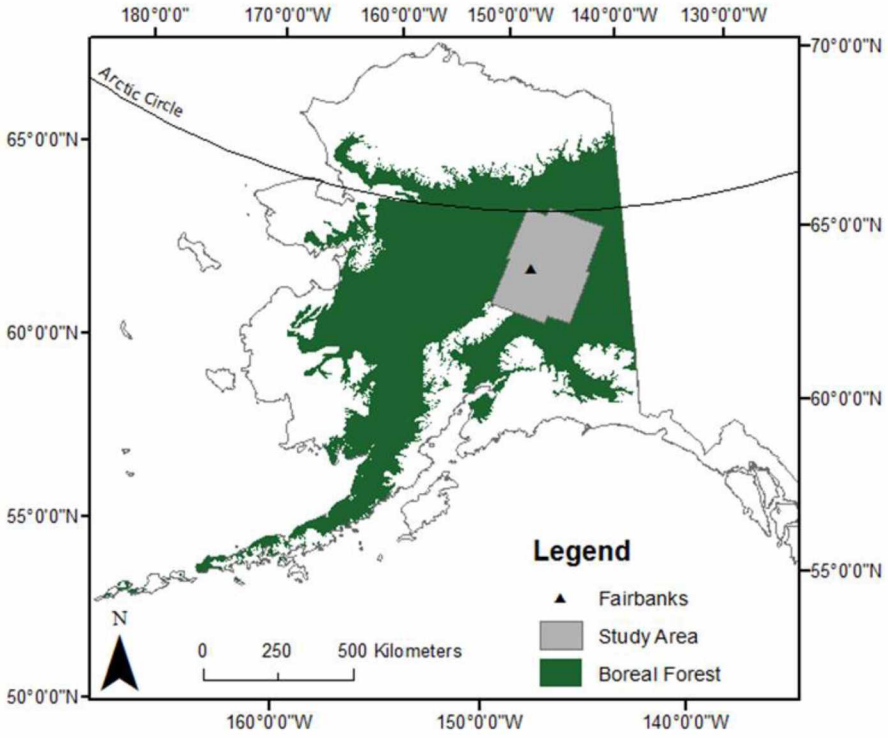

Figure 1. Study area location map. The study area lies just below the Arctic Circle and covers 93,610 km^2.

1.4.2. Study Area Description

The study area spans from the Yukon River just south of Fort Yukon, to the southern border of the Alaska Range, covering a total of 93,610 km^2. The boreal forest consists of primarily nine tree species, the following of which dominate the region: black spruce (*Picea mariana*), white spruce (*Picea. glauca*), alder (*Alnus tenuifolia*), paper birch (*Betula neoalaskana*), aspen (*Populus tremuloides*), and balsam poplar (*Populus balsamifera*). The forest has a simple structure with either a single layer closed canopy, or an open canopy stand. The understory usually consists of mosses (*Sphagnum spp.*) and shrubbery (*Betula nana*, *Ledum palustre*, *Vaccinium spp.*) (Ustin and Xiao, 2001). This area is of interest not only because it is located within the boreal forest, but also because the University of Alaska Fairbanks and the Bonanza Creek Long Term Ecological Research (BNZ-LTER) Network are located within it and they are both major hubs for Arctic/Sub-Arctic research.

1.4.3. Vegetation Classes

In this study a total of 9 vegetation classes were defined using a modified classification system of the 2001 USGS NLCD classification system, which is modified from the Anderson Land Cover Classification System (Homer et al., 2007; Anderson, 1976). The vegetation classes used, shown below in Table 1, are consistent with USGS NLCD vegetation classes. In addition to the vegetation classes, barren land, open water, and ice/snow categories also consistent with the classes in the USGS NLCD products were classified.

Table 1. Vegetation Classes. Adapted from Homer et al., 2007.

Class\Value	Vegetation Class
Forest	
1	**Deciduous Forest**
2	**Evergreen Forest**
3	**Mixed Forest**
Shrubland	
4	**Dwarf Shrub**
5	**Shrub/Scrub**
Herbaceous	
6	**Sedge**
7	**Grassland**
Wetlands	
8	**Woody Wetlands**
9	**Emergent Herbaceous Wetlands**
Barren Land	
10	**Barren Land (Rock/Sand/Clay)**
Water	
11	**Open Water**
12	**Ice/Snow**

Deciduous Forest (Figure 2) is described as areas dominated by trees generally greater than 5 meters tall, and greater than 20% of total vegetation cover. More than 75% of the tree species shed foliage simultaneously in response to seasonal change.

Figure 2. Example of a deciduous forest (From Boggs et al., 2012).

Evergreen Forest (Figure 3) is described as areas dominated by trees generally greater than 5 meters tall, and greater than 20% of total vegetation cover. More than 75% of the tree species maintain their leaves all year. Canopy is never without green foliage.

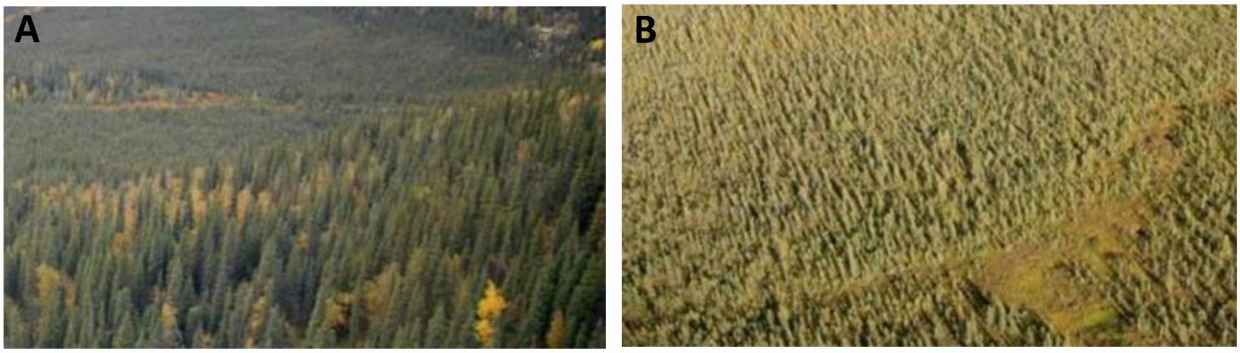

Figure 3. Examples of evergreen forests. A) White spruce dominated forest. B) Black spruce dominated forest (From Boggs et al., 2012).

Mixed forest (Figure 4) is described as areas dominated by trees generally greater than 5 meters tall, and greater than 20% of total vegetation cover. Neither deciduous nor evergreen species are greater than 75% of total tree cover.

Figure 4. Example of a mixed forest (From Boggs et al., 2012).

Dwarf Shrub (Figure 5) is described as areas dominated by shrubs less than 20 centimeters tall with shrub canopy typically greater than 20% of total vegetation. This type is often co-associated with grasses, sedges, herbs, and non-vascular vegetation.

Figure 5. Example of a dwarf shrub dominated area (From Boggs et al., 2012).

Shrub (Figure 6) is described as areas dominated by shrubs; less than 5 meters tall with shrub canopy typically greater than 20% of total vegetation. This class includes true shrubs, young trees in an early successional stage or trees stunted from environmental conditions.

Figure 6. Examples of shrubland (From Boggs et al., 2012).

Sedge (Figure 7) is described as Alaska only areas dominated by sedges and forbs, generally greater than 80% of total vegetation. This type can occur with significant other grasses or other grass like plants, and includes sedge tundra, and sedge tussock tundra.

Figure 7. Example of a sedge dominated landscape (From Boggs et al., 2012).

Grassland (figure 8) is described as areas dominated by graminoid or herbaceous vegetation, generally greater than 80% of total vegetation. These areas are not subject to intensive management such as tilling but can be utilized for grazing.

Figure 8. Example of grassland (Boggs et al., 2012).

Woody wetlands (Figure 9) are described as areas where forest or shrubland vegetation accounts for greater than 20% of vegetative cover and the soil or substrate is periodically saturated with or covered with water.

Figure 9. Example of a woody wetland (Boggs et al., 2012).

Emergent Herbaceous Wetland (Figure 10) is described as areas where perennial herbaceous vegetation accounts for greater than 80% of vegetative cover and the soil or substrate is periodically saturated with or covered with water.

Figure 10. Example of emergent herbaceous wetlands (From Boggs et al., 2012).

Barren Land (Figure 11) is described as areas of bedrock, desert pavement, scarps, talus, slides, volcanic material, glacial debris, sand dunes, strip mines, gravel pits and other accumulations of earthen material. Generally, vegetation accounts for less than 15% of total cover.

Figure 11. Example of barren land (From Boggs et al., 2012).

2. DATA

2.1. Remote Sensing and Ancillary Data

Level 1 surface reflectance Landsat images were selected to use in the making of the vegetation maps due to several factors such as: (1) comparability with the USGS NLCD products, (2) availability of images dating back to the 1980s, (3) suitability of the 30 meter spatial resolution for vegetation classification, and (4) free and easy accessibility of Landsat-4-5 Thematic Mapper (TM) and Landsat-8 Operational Land Imager (OLI) images, courtesy of the U.S. Geological Survey.

Landsat 1 was first launched in 1972, and aboard it was the Multispectral Scanner (MSS). Since then, there have been six more successful satellites launches. Landsat 2 launched in 1995 and Landsat 3 launched 1978, both of which also carried the MSS. The launch of Landsat 4 followed in 1982, and then Landsat 5 in 1984, both of which had an update to the TM as well as carrying the MSS. Landsat 7 launched in 1999 had an Enhance Thematic Mapper (ETM+). Lastly, Landsat 8 was launched in 2013 carrying the Operational Land Imager (OLI). The suite of Landsat satellites provides the longest record of continuous satellite imagery, more than 40 years, for monitoring the Earth's land processes from space at medium resolution. It has been demonstrated through numerous studies that the combination of spatial and spectral resolutions of Landsat sensors (Table 2) make it a good source of remote sensing images for vegetation/land cover mapping (Basham May et al., 1997; Cingolani et al., 2004; Harvey and Hill, 2001; Kussul et al., 2015; Wolter et al., 1995; Zhao et al., 2015 and others), especially studies related to observing long term changes to the Earth's surface (Xie et al., 2008).

*Table 2. Landsat 4-5 TM and Landsat 8 OLI spectral and spatial resolution. *The thermal band was acquired at 120 m resolution but resampled to 30 m pixels*

Satellite	Bands	Wavelength (μm)	Spatial Resolution (m)
Landsat 4-5 TM	Band 1 - Blue	0.45 - 0.52	30
	Band 2 - Green	0.52 - 0.60	30
	Band 3 - Red	0.63 - 0.69	30
	Band 4 - Near Infrared	0.76 - 0.90	30
	Band 5 - Shortwave Infrared (1)	1.55 - 1.75	30
	Band 6 - Thermal	10.40 - 12.50	120*
	Band 7 - Shortwave Infrared (2)	2.08 - 2.35	30
Landsat 8 OLI	Band 1 - Ultra Blue	0.435 - 0.451	30
	Band 2 - Blue	0.452 - 0.512	30
	Band 3 - Green	0.533 - 0.590	30
	Band 4 - Red	0.636 - 0.673	30
	Band 5 - Near Infrared	0.851 - 0.879	30
	Band 6 - Shortwave Infrared (1)	1.566 - 1.651	30
	Band 7 - Shortwave Infrared (2)	2.107 - 2.249	30

Images used for the 1985, 1995, or 2005 vegetation classification maps were Landsat 4/5 TM surface reflectance products at 30 meter spatial resolution. All images used for the 2015 vegetation classification map were Landsat 8 OLI surface reflectance products at 30 meter spatial resolution. Surface reflectance products were chosen because they are atmospherically corrected and can be directly compared to spectral curves collected either from ground measurements or other instruments (Masek et al., 2006). Individual images were selected based on the amount of cloud cover, with perfectly clear images being optimal. Images were then further narrowed down by the amount of greening in the images, classified as either leaf on or leaf off (with leaf on being preferred in the use of the final product, but leaf off used to distinguish between deciduous and evergreen during visual interpretation). The specifications of each scene used to generate the maps, including their World Reference System (WRS) path and row numbers, are displayed in Table 3 below.

A Digital Elevation Model (DEM) of the area was acquired from the USGS National Elevation Dataset (NED) (accessed at https://nationalmap.gov/elevation.html). The NED is a continuous

raster elevation product for the conterminous United States, Alaska, Hawaii, and the island territories, and represents the best available elevation data for the large area coverage, with source data from both public and private entities. For the conterminous United States, the grid spacing is 1-arc-second, or approximately 30 meters. For the state of Alaska, lower resolution source data resulted in the use of 2-arc-second grid spacing, or 60 meter resolution (Gesch et al., 2002). The DEM was resampled to 30 meter resolution, and slope and aspect files were created in ArcGIS from the DEM and were also used as input into the classification procedure.

Table 3. Landsat Scene Specification. Each scene used was the least cloudy image for that path and row within the decade. Data acquired in mm/dd/yyyy format.

Lansat Scene ID	Spacecraft ID	Sensor ID	WRS Path	WRS Row	Date Aquired	Cloud Cover (%)
1985 Map						
LT50680141985213XXX09	Landsa t 5	TM	68	14	8/1/1985	0
LT50680151987235XXX01	Landsat 5	TM	68	15	8/23/1987	9
LT50690141984266PAC02	Landsat 5	TM	69	14	9/22/1984	0
LT50690151984266PAC06	Landsat 5	TM	69	15	9/22/1984	3
1995 Map						
LT40680141993195XXX01	Landsat 4	TM	68	14	7/14/1993	10
LT40680151993195XXX02	Landsat 4	TM	68	15	7/14/1993	0
LT50690141991173XXX02	Landsat 5	TM	69	14	6/22/1991	2
LT50690151991173XXX04	Landsat 5	TM	69	15	6/22/1991	9
2005 Map						
LT50680142003199PAC03	Landsat 5	TM	68	14	7/18/2003	0
LT50680152003199PAC03	Landsat 5	TM	68	15	7/18/2003	1
LT50690142006246PAC01	Landsat 5	TM	69	14	9/3/2006	7
LT50690152003222PAC02	Landsat 5	TM	69	15	8/10/2003	2
2015 Map						
LC80680142014261LGN01	Landsat 8	OLI_TIRS	68	14	7/13/2013	1
LC80680152013194LGN01	Landsat 8	OLI_TIRS	68	15	7/13/2013	3
LC80690142013169LGN01	Landsat 8	OLI_TIRS	69	14	6/18/2013	7
LC80690152013169LGN01	Landsat 8	OLI_TIRS	69	15	6/18/2013	5

Four Landsat scenes cover the study area (see Figure 12 and 13). Although the scenes can be identified by their WRS path and row, from this point on they may also be referred to as the northeast, northwest, southeast, or southwest scenes for ease of reference.

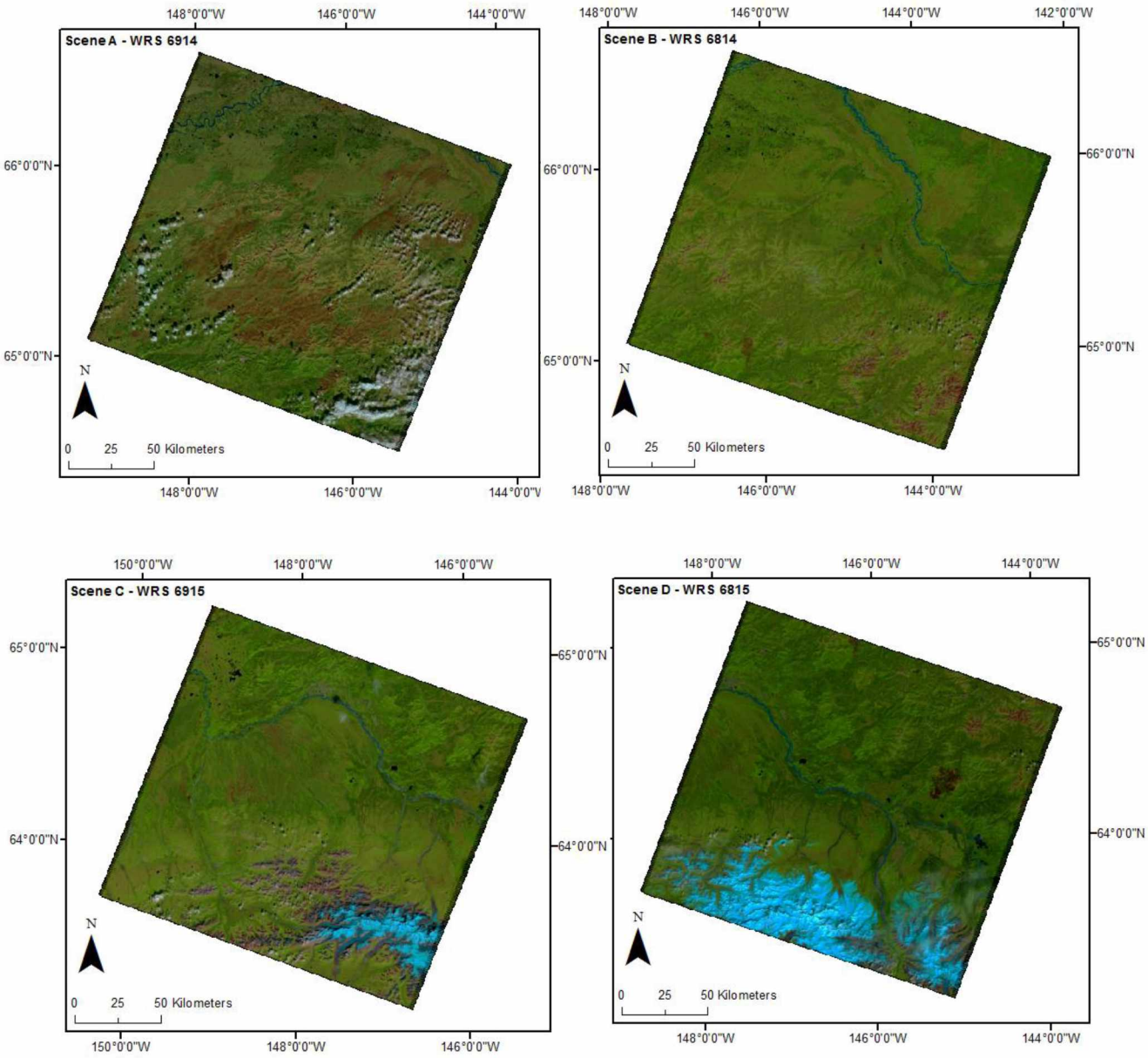

Figure 12. Landsat scene locations. Scenes are displayed as a false natural color composite with shortwave medium infrared, near infrared, and red bands displayed as red, green, and blue, respectively.
Northwest Scene: WRS 69-14
Northeast Scene: WRS 68-14
Southwest Scene: WRS 69-15
Southeast Scene: WRS 68-15

The geographic location of the study area and the orbiting paths of the Landsat satellites creates significant overlap between the scenes (Figure 13). The order of the overlap varies with each map, depending on the cloudiness of the individual scenes, with the clearest scenes being displayed in front.

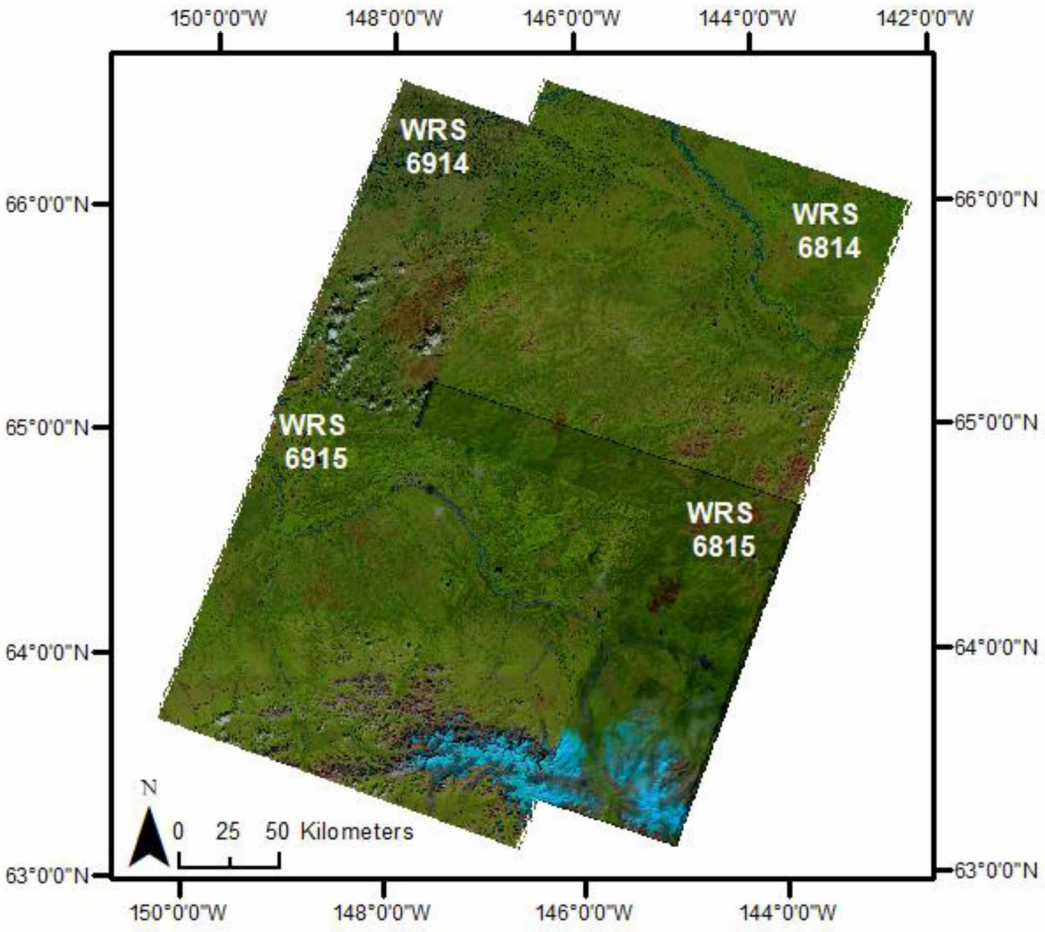

Figure 13. Landsat scene overlap. Landsat scenes displayed in a false natural color composite. The displayed configuration is for the 2005 map, but the order of overlap varies between each map, depending on cloudiness.

2.2. Field Data

Field data was used from two different sources and was split into two parts a) as training data for the vegetation classification, and b) testing data for the model evaluation. The first was from the Bonanza Creek Long Term Ecological Research (BNZ-LTER) Network, which provided

us with all their known vegetation plots. All the ground-truth information from the BNZ-LTER was collected through field observation (Hollingsworth, 2010). The second set of ground-truth training data came from the public LANDFIRE Reference Database (LFRDB) provided by the LANDFIRE Program (LANDFIRE, 2001). The LFRDB is a compiled dataset that includes all existing georeferenced field data available for the United States that has been made available to the public and is collected from both government and nongovernment sources. This information goes through a series of quality controls, such as satellite image overlay and comparison to digital photographs when available (Rollins, 2009). Both datasets included latitude and longitude locations of an area of known vegetation type, a description of the area, and the year the data was collected. Both datasets were clipped to the area of interest and projected into the default coordinate system of the Landsat scenes, UTM Zone 6 North with a WGS 84 datum. The ground truth data points were sorted into one of the 9 vegetation cover types by their site description. With both data sets combined, there were nearly 4,000 ground truth points. Figure 14 below shows the distribution of all available field data within the study area.

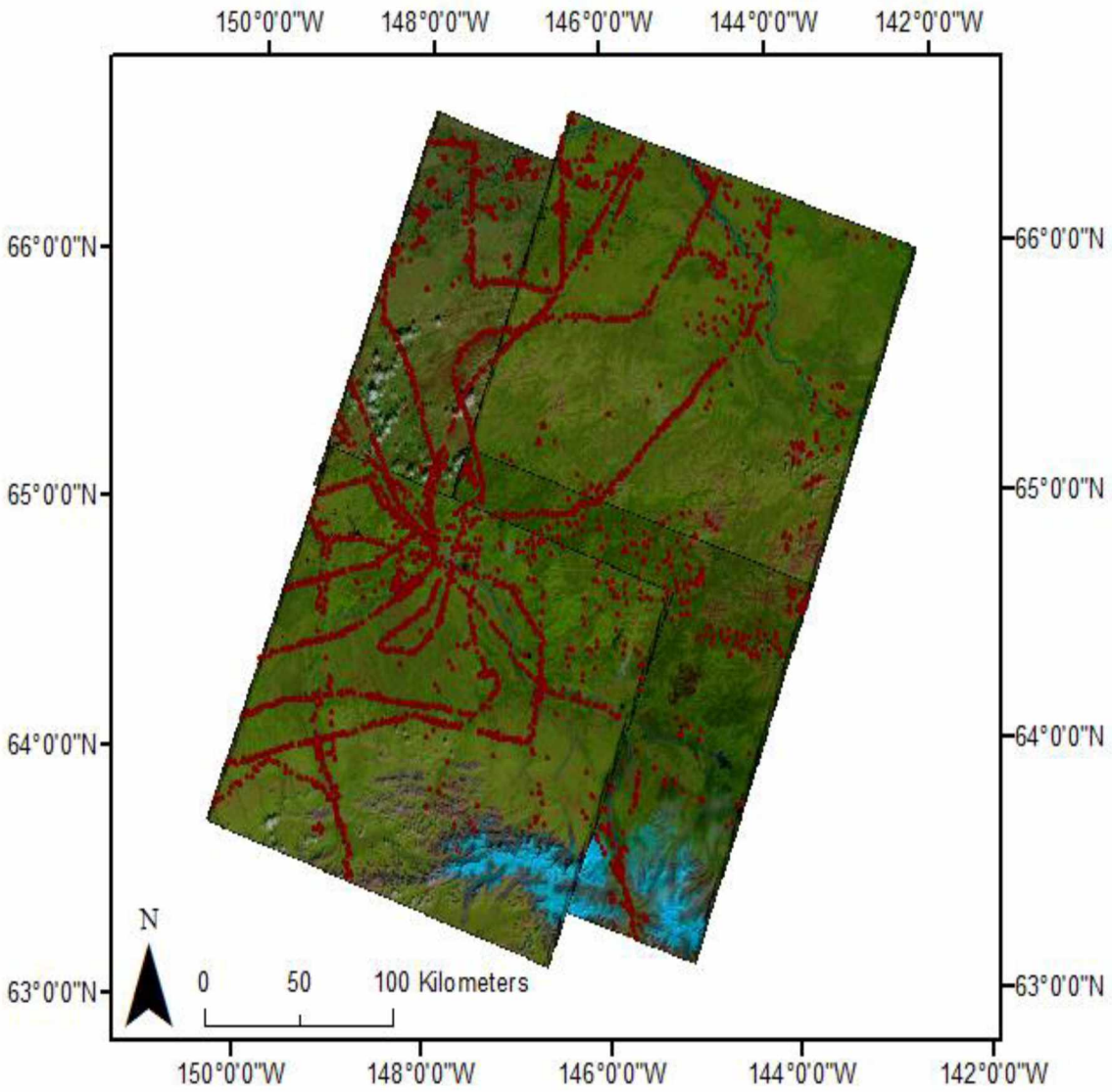

Figure 14. Distribution of all available field data shown in red. 20% of this field data will be withheld for model accuracy assessments.

3. METHODS

The sequence for the pre-processing, classification processing and the post-processing is shown below in Figure 15. The field data required much more pre-processing work than the remote sensing imagery.

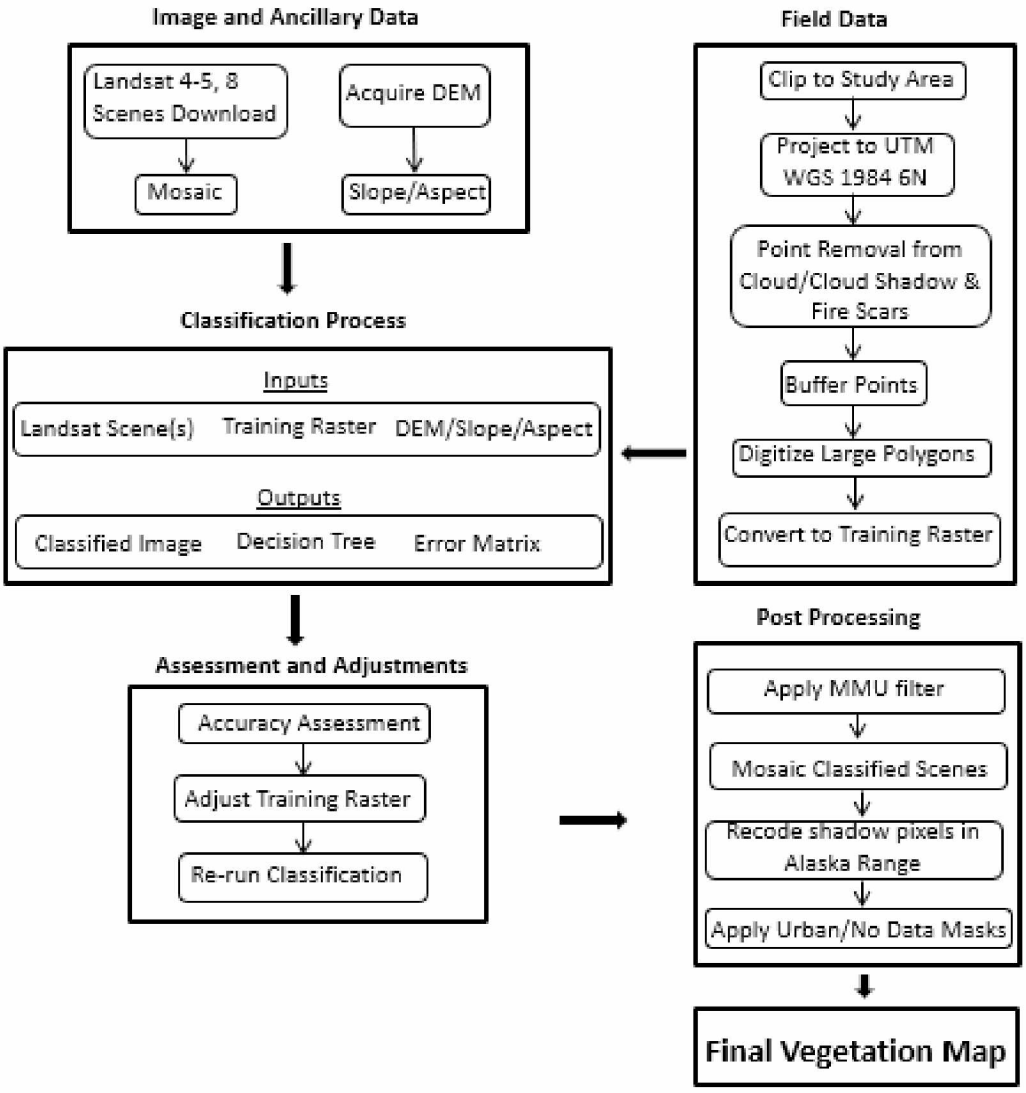

Figure 15. Methodology flow chart: This flow chart shows the process to complete one vegetation map. This process was repeated three more times to generate the four vegetation maps. Comparative analysis of multitemporal vegetation maps occur after all vegetation maps are generated.

3.1. Pre-processing

A large amount of preprocessing was required before scenes could be classified. Images that were acquired on the same day were mosaicked using ERDAS Mosiac Pro with the automatic weighted seamlines. Weighted seam lines are automatically generated by a weighted combination of color and gradient similarities to find the locations with high similarity (Yu et al., 2012). Once the ground truth data was clipped to the study area, all points that were lying under cloud cover or cloud shadow were removed. Cloud cover and cloud shadow were identified using visual interpretation, paying close attention to color, texture, and shape. Cloud shadows were easily identified due to their dark, almost black, color in a false natural color composite, where the first shortwave infrared band (SWIR-1) is displayed in red, near infrared (NIR) band is displayed in green and red band is displayed as blue. Clouds were more easily identified in a custom band combination where the blue band is displayed in red, the green band is displayed in green, and the SWIR-1 band is displayed in blue. A comparison of the false natural and false color composites is displayed in Figure 16. The clouds appear a much brighter white where the background appears a dark blue color compared to the false natural color composite. A broad cloud mask was manually digitized for each scene and used to remove the points.

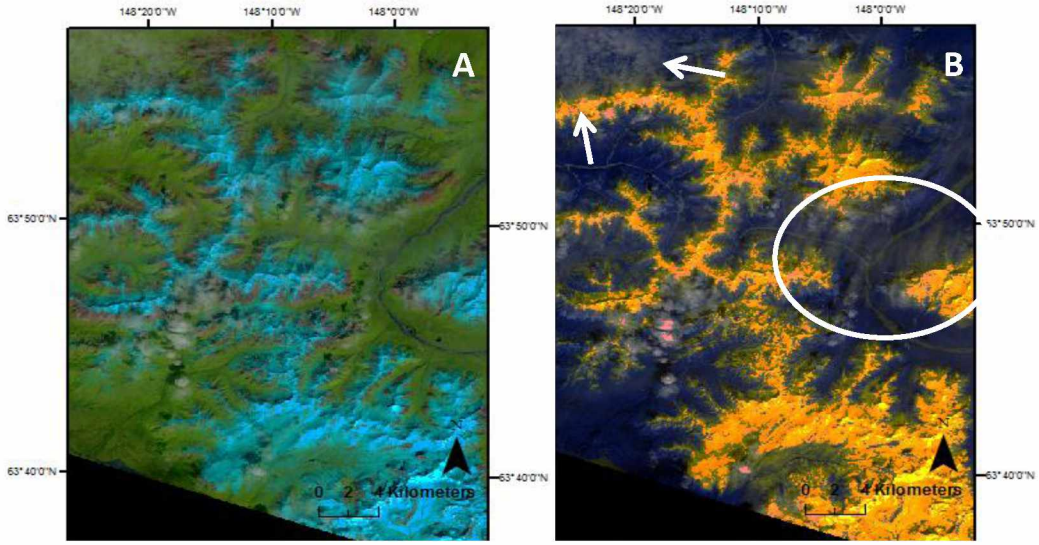

Figure 16. False natural and false color composite comparison. A) False natural color composite B) False color composite. Thinner, hazy clouds and clouds above the mountains are more easily identified in the false color composite in white.

As Figure 17 shows, forest fire is the largest natural disturbance in the state of Alaska (LANDIRE, 2012b). A subset of training points that were not located within any fire scars (fire boundaries provided by the Alaska Interagency Coordination Center and housed at the Alaska Fire Science Consortium) from 1980-2017 were used as the base training set for all images, because without fire disturbances, these areas were likely to go unchanged.

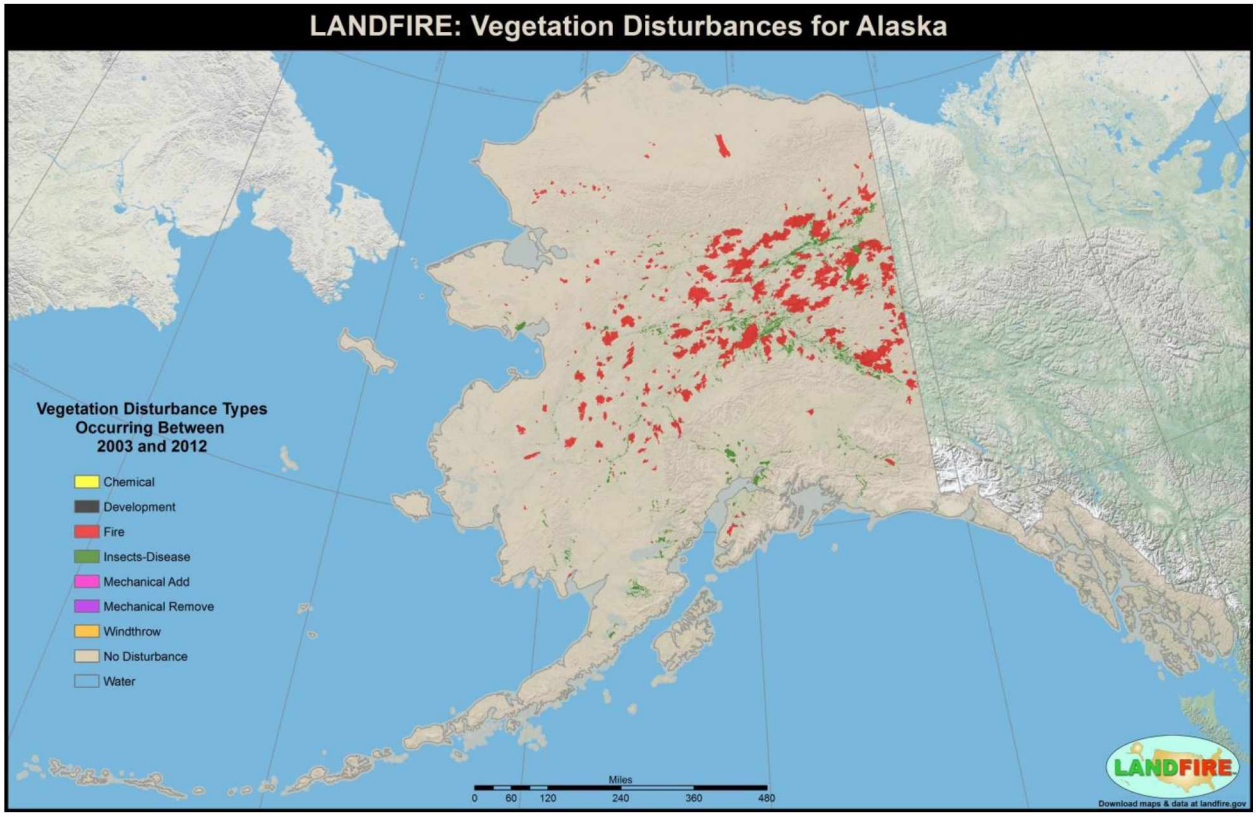

Figure 17. Vegetation disturbances for Alaska. Fire is represented in red, and is by far the largest disturbance agent for vegetation in interior Alaska (From LANDFIRE, 2012b).

These points were buffered with a radius distance of 150 meters and then converted to polygons to increase the number of training pixels in each scene. This specific buffering distance was reached through a series of trial and error where a smaller buffering distance did not provide enough training pixels, and a larger buffering distance had too many points of different classes overlapping. Any polygons overlapping bodies of water were removed. To further increase the amount of training information in each scene, large polygons of the following classes were manually digitized and used as training data: open water, ice/snow, deciduous forest, evergreen

forest, and barren land. These polygons were created using visual interpretation. Open water, ice/snow, and barren land polygons were digitized by looking at the original imagery as these classes are easily identified in the imagery by their color, texture, and shape. Deciduous and evergreen polygons were created while comparing a leaf-off scene to the original. Up until this point, all information was a combination of tabular and vector data. The last step before classification was conversion to a raster training dataset. If an overlap of classes occurred within the same raster cell, the class with the most instances determined the value for that cell.

The first map to be completed was the 2005 map, as the USGS NLCD 2001 map could be used as a good comparative baseline. A set of training data was completed for each Landsat scene for the 2005 map following the methods described above. The base set of training data for each scene was then adjusted for all the following scenes in the 1985, 1995, and 2015 maps. Because maps still needed to be completed for time windows before and after the base map, the base sets of training data needed to be adjusted. For the 1985 and 1995 classified images, there were points in the training set that were removed because of fires scars that were present in the 2005 classified image but occurred after the acquisition date of the new Landsat imagery (i.e. points that were located in burn scars in the 1990s needed to be removed for the 2005 time period but could still be used for the 1985 time period). These points were buffered and supplemented back into the scene. Conversely, there were points that were located in fire scars occurring after the acquisition data of the Landsat imagery for the 2005 classified image, but before the acquisition date of the new 2015 Landsat imagery (i.e. any points within fires scars before 2013 were no long suitable for the 2015 classified image). These points were removed. The larger digitized polygons of open water, ice/snow, deciduous forest, evergreen forest, and barren land were visually checked to see if they still fit the scenes and were removed or adjusted to reflect the changes between the scenes. For example, the two braided rivers throughout the study area were continually changing throughout the years, with channels changing width and shape. Digitized polygons of open water along the river channels needed to be adjusted for each scene to account for the changing shape of the braided channels.

3.2. Classification Process

A decision tree (DT) software, See5 (the Windows version of the Linux C5 software), was used to run the classification process (Quinlan 1993). DT is a supervised prediction method that partitions data values into predefined sets of classes by their attribute values. DTs rely on training sets for their machine learning, and a positive correlation exists between training sets and predictive performance (Rokach and Maimon, 2008). DTs are composed of nodes and branches. There are three different types of nodes; the root node which contains the decision that will further subdivide all records into a minimum of two mutually exclusive subsets, the internal nodes which split the data into one of the remaining available choices at that location in the tree, and the leaf nodes which represent the final outcome after the combination of prior decisions. The branches represent the outcomes that originate from the previous node. The branches follow a hierarchy and can be represented by if-then rules (Song and Ying, 2015).

See5 uses an adapted form of the gain criterion, Equation 1, known as the information gain ratio, Equation 2, which adjusts for the bias of test results with many outcomes resulting from the gain criterion.

$$split\ info(x) = -\sum_{i=1}^{n} \frac{T_t}{T} \times log_2\left(\left|\frac{T_t}{T}\right|\right)$$

Equation 1.The potential information generated by dividing training classes, T, into subsets n. The information relevant to classification that comes from this same division is known as the information gain (From Quinlan 1993).

$$gain\ ratio(X) = \frac{gain(X)}{split\ info(X)}$$

Equation 2.The gain ratio conveys the useful information for the classification generated by the split (From Quinlan 1993).

This maximizes the proportion of information that appears helpful for the classification (Homer et al., 2004; Quinlan 1993). See5 also offers a pruning algorithm, reduced error, to ensure overfitting of the training data does not happen. First, the decision tree is grown so that all training samples

are classified correctly. Then, error rates of the tree on a set of unseen separate cases are assessed. The tree is 'pruned' by removing leaf nodes that are fit to noise in the training data and are predicted to have high error rates. This is done by working from the bottom of the tree up, replacing internal nodes with the most frequent class if accuracy is not reduced (Friedl and Brodley, 1997; Homer et al., 2004; Quinlan 1993; Rokach and Miamon, 2008). Adaptive boosting is an advanced feature that See5 is equipped with based on the work of Freund and Schapire (1996). Several decision trees are generated, and each consecutive tree pays close attention to the mistakes regarding certain classes in order to correct them. Each class is initially weighted equally, but after the first iteration, comparison of the classification output and the labels for each class uncover classes that have been classified incorrectly. These weaker classes are given an increased weight and the algorithm is run again. The iterations continue until the trials reach very good or very poor results, or until the set number of iterations is complete (Pal and Mather, 2003; Quinlan, 1996). In this study, a 10-classifier boosting (10 iterations) was used, which on average results in a reduction between 10-19% of the classification error (Quinlan, 1996). Another advanced feature See5 contains is cross validation. For this study the training data set is divided into 10 subsets of equal size to conduct a 10-fold cross validation. The model is run 10 times, each time an accuracy assessment is derived one subset is used to evaluate the accuracy assessment derived from the other 9 subsets. Although cross validation is used to describe estimates of model prediction accuracy, this type of validation is only a first order estimate of data quality, not a formal accuracy assessment. The logic behind this is addressed in more detail in section 4.2 (Homer et al., 2007).

Other types of classifiers were considered for the classification, such as spectral clustering or artificial neural networks, but ultimately the decision tree algorithm was preferred over the other methods of classification. Decision tree has the following advantages over other types of classifiers (Homer et al., 2007): its independence of the distribution of class signatures from its non-parametric nature, its ability to work with nominal and continuous data, its generation of readable and interpretable classification rules, its speed in training, and its performance (often slightly more accurate compared to the previously mentioned classifiers).

ERDAS Imagine, along with a See5 plug in and an interface designed to generate classified pixels from DT models generated by USGS was used for the classification process and ran on a Windows 10 operating system (Homer et al., 2001). In this study, 80% of ground truth data was used for classification, and 20% was withheld for the model evaluation. The sample method for all training data was stratified random. Independent inputs into the software were always the image (or mosaicked image) and the DEM and/or slope/aspect file, and the training raster was always the dependent variable. Several iterations through the software, along with adjustments to the training data (increasing or decreasing the number or sizes of digitized areas of classes), were needed to improve classification accuracy for each scene.

3.3. Post-processing

Four different types of post-processing procedures were needed after the classification process. This first type was a "smart eliminate aggregation algorithm" generated by the USGS. This algorithm aggregated to a one acre (five pixel) minimum mapping unit using eight corner connectivity from a central pixel and made a "smart" decision on a dissolve protocol based upon a weighting table. This particular algorithm allows corner and square (queen and rook), or 8 pixels connectivity to count giving equal weight to both. This allows for nonlinear features, such as streams, to remain intact. The smart eliminate algorithm is designed to remove only noise, such as the salt and pepper effect, and retain the exact look and feel, as where these features could be dissolved out by traditional clump and sieve filters. For example, a braided stream running northwest to southeast undergoing this algorithm will remain touching only the corners (Homer et al., 2001).

The second type is manual editing due to the long shadows introduced throughout the mountainous region of the Alaska Range near the bottom of southwest and southeast scenes. These shadows are often classified as open water or evergreen vegetation classes, although they

were clearly mapped over the glaciated areas in the Alaska Range, and should have been classified as ice/snow. These pixels were manually recoded to their correct ice/snow class.

The third post-processing procedure was in the form of a mask. Two different masks were applied to the final vegetation map products. The first was the no data mask (i.e. areas with insufficient data to be classified were masked). Although training data was removed in areas of clouds or cloud shadows with a manually digitized broad cloud mask, these features remained present in the image while the classification was being processed. For this reason, a cleaner and tighter fitting mask was generated where clouds and cloud shadows completely covered the ground surface from view, or interfered with the classification process, resulting in incorrect or no data for the classification. These tighter masks were created with an algorithm called Fmask when possible (Zhu et al., 2015; Zhu and Woodcock, 2012). The USGS uses a derivative (conversion to C code) of this software called CFMask in creating their Landsat Level 1 Collection 1 quality assessment band (Foga et al., 2017). The version used in this study is newer (4.0 vs 3.3) and runs on a Windows 10 operating system (download and more information available at https://github.com/prs021/fmask). The masks created for the southwest and southeast scenes were manually adjusted when ice/snow was picked up as cloud and when the shadows created by the Alaska Range were confused for shadow. In the case of thin clouds, visual interpretation was used to check if the translucent or hazy clouds interfered with the classification or not and were masked if they did.

The fourth post-processing step was applying the second mask, an urban mask, to the final vegetation products. Although the following maps are vegetation maps, there is one heavily populated area within the study area. The urban impervious surfaces mask was created by clipping the image to the extent of the urban area and running a separate supervised classification (much simpler than the detailed vegetation classification) in ERDAS Imagine with the following broad classes: urban, water, and vegetation. Since the study area has only one significant urban area, the urban mask covers all impervious surfaces and is not separated into the amount of development like the USGS NLCD maps.

4. RESULTS

This chapter contains the results from the classification methodology work flow of the four vegetation maps for the study area for the nominal years of 1985, 1995, 2005, and 2015. The error matrix and user's and producer's accuracies for each scene or mosaicked scenes are also presented. The overall accuracy for each scene, as well as an overall weighted accuracy for each map has been generated. The distribution of the 9 vegetation classes (plus open water, ice/snow and barren land) for each map is also displayed. Lastly, cross tabulation tables were generated between the years of 1985-2015, and 1995-2015.

4.1. Vegetation Classification Maps

4.1.1. 1985 Vegetation Classification Map

For the 1985 vegetation map, the northwest and southwest scenes were mosaicked together because they were acquired on the same day of the same year. These two scenes had the latest acquisition date in the season out of all the images for all the maps, September 22nd. By this time in Alaska, it is likely that the deciduous trees had lost a good amount of their foliage. This is further discussed in Chapter 5. The northeast and southeast scenes were also mosaicked together, even though they were not acquired on the same day or even the same year, because they were similar enough in their phenology.

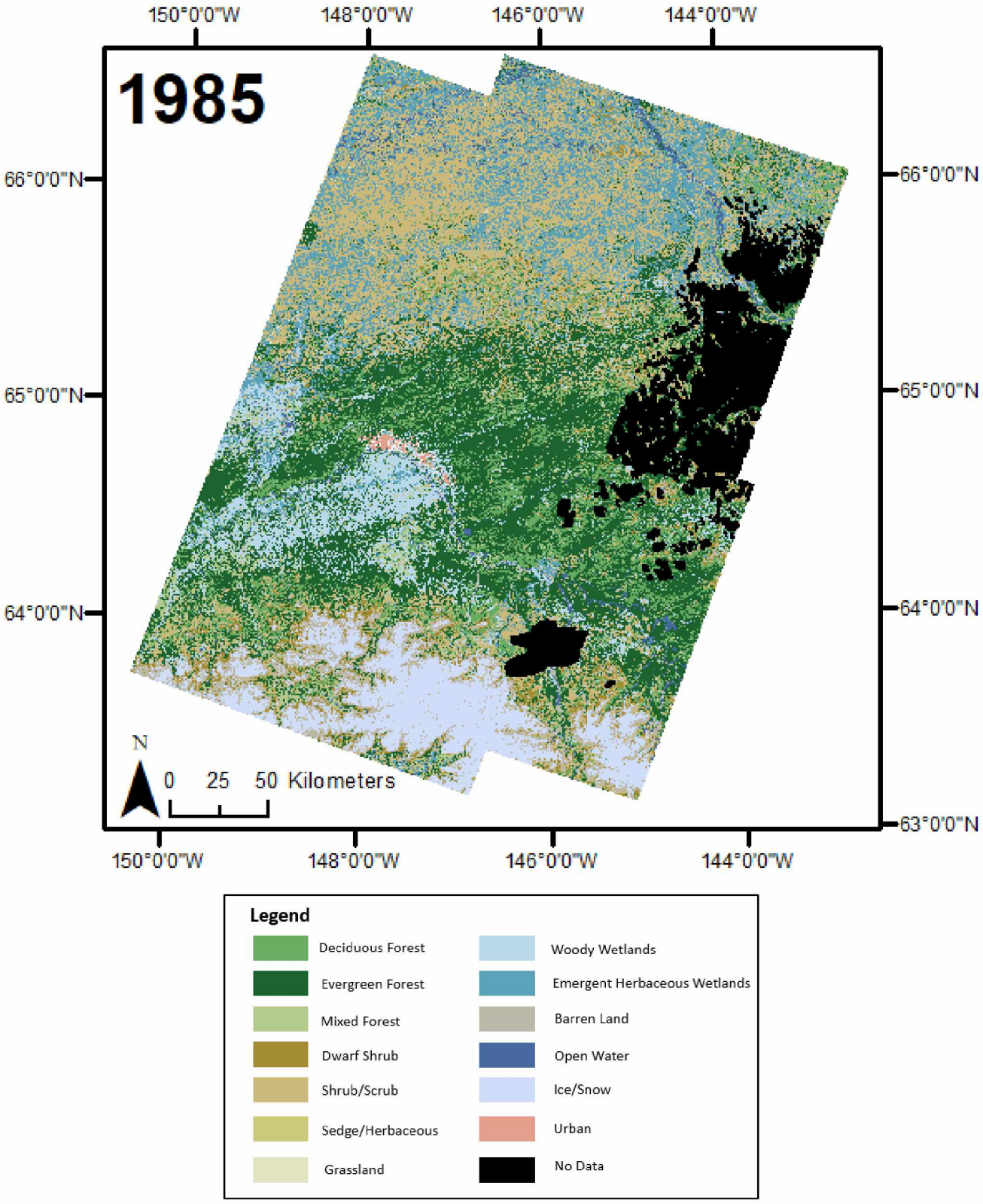

Figure 18. 1985 Vegetation Map. Because of the later acquisition date for the southwest scene, this map has the most extensive snow cover.

4.1.2. 1995 Vegetation Classification Map

For the 1995 map, the northwest and southwest scenes mosaicked, as well as the northeast and southeast scenes. The decade of the 1990's was the most difficult to find cloud free imagery, resulting in this map having the most cloud coverage of all the maps, even though the clearest images for each WRS path and row from this decade were selected.

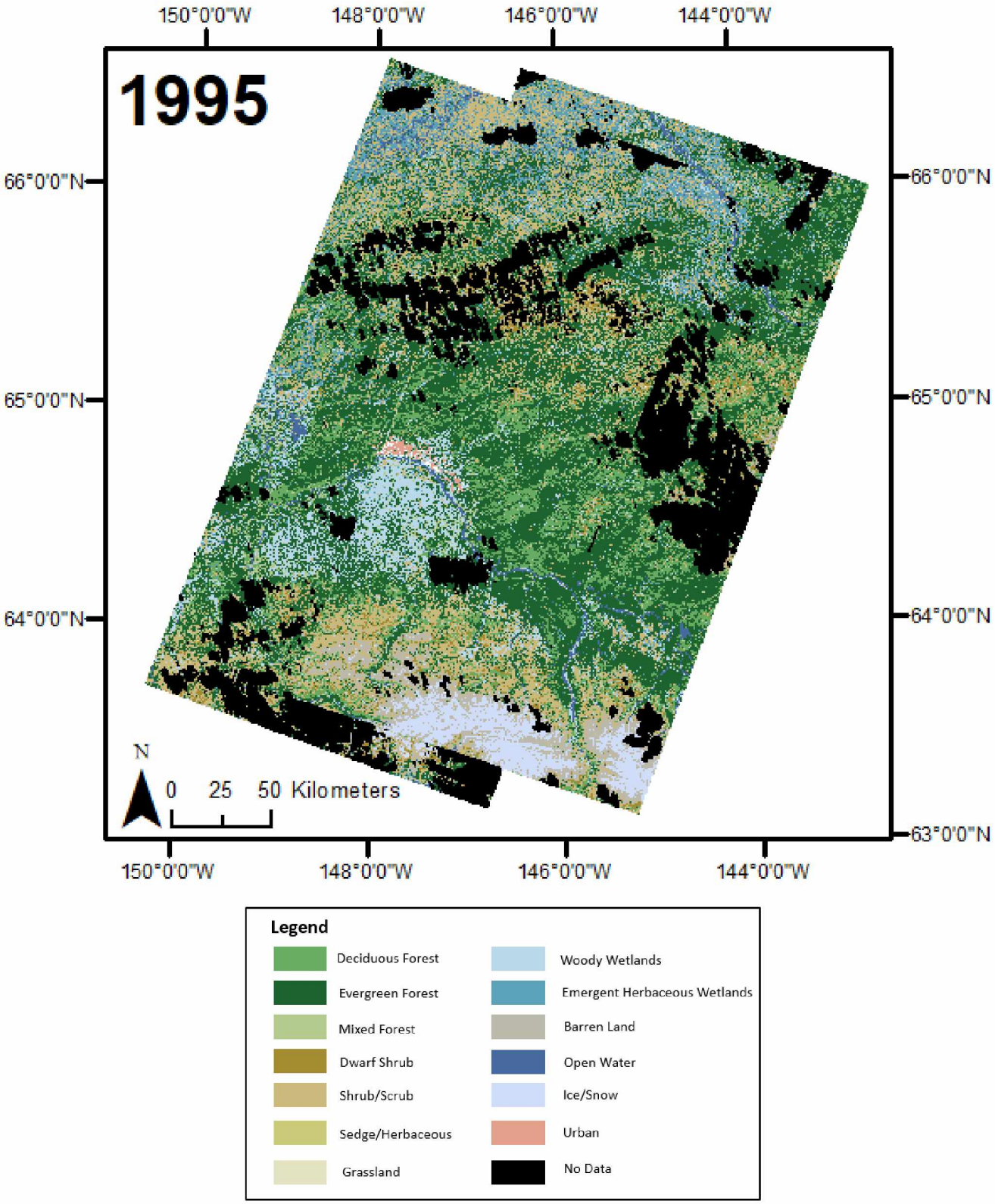

Figure 19. 1995 Vegetation Map. The most cloud covered map from this study.

4.1.3. 2005 Vegetation Classification Map

The northeast and southeast scenes were mosaicked together for the 2005 vegetation cover map. This was the first vegetation map to be completed and served as the base map for this study. Several iterations through the classification process were required for each scene in this map to get a good base training set for each scene.

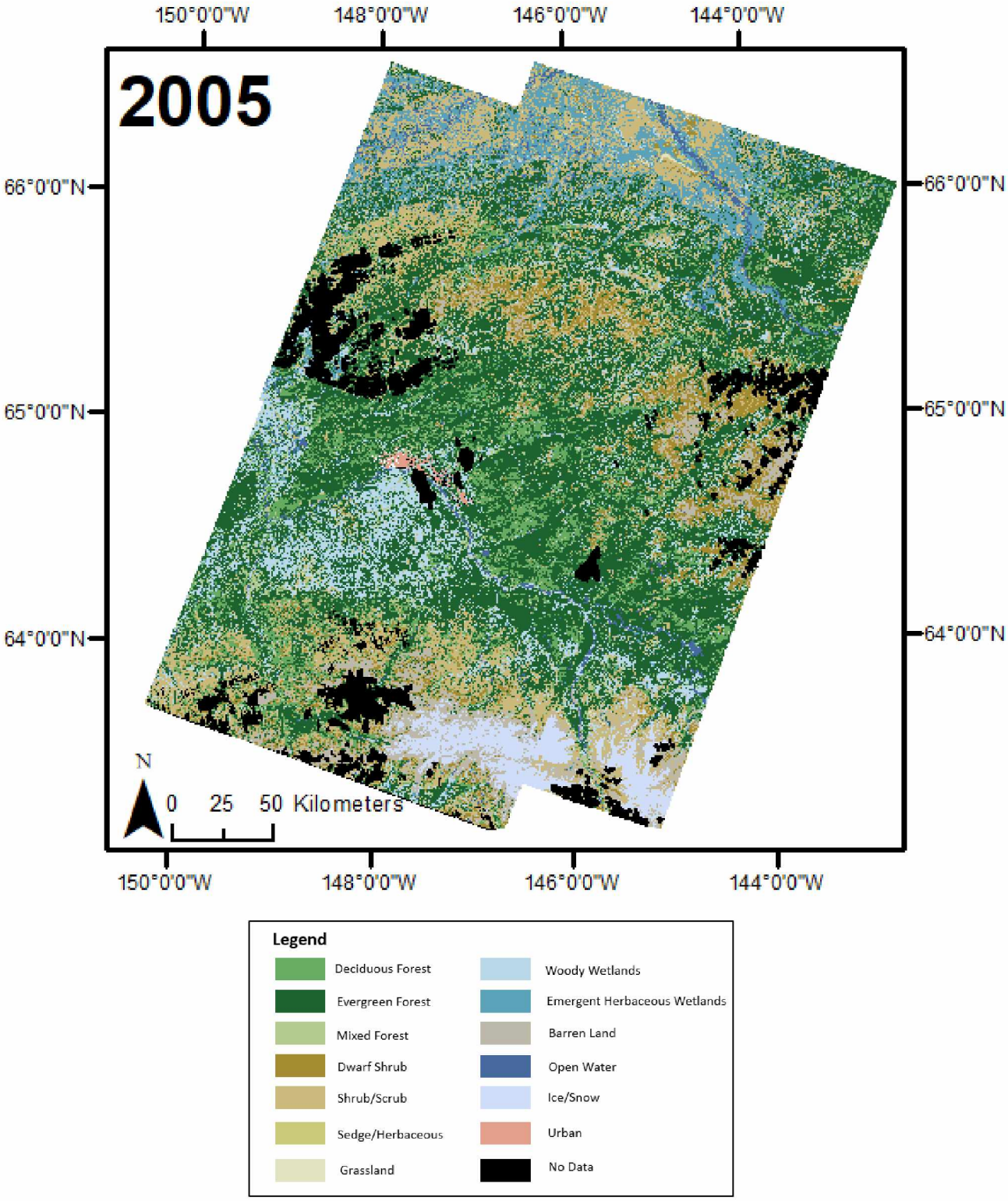

Figure 20. 2005 Vegetation Map. The base map for this study.

4.1.4. 2015 Vegetation Classification Map

The northwest and southwest scenes, as well as the northeast and southeast scenes were mosaicked together to generate this map. This decade had the most cloud free images available compared to the other three but finding perfectly clear images for the area of study was still a challenge.

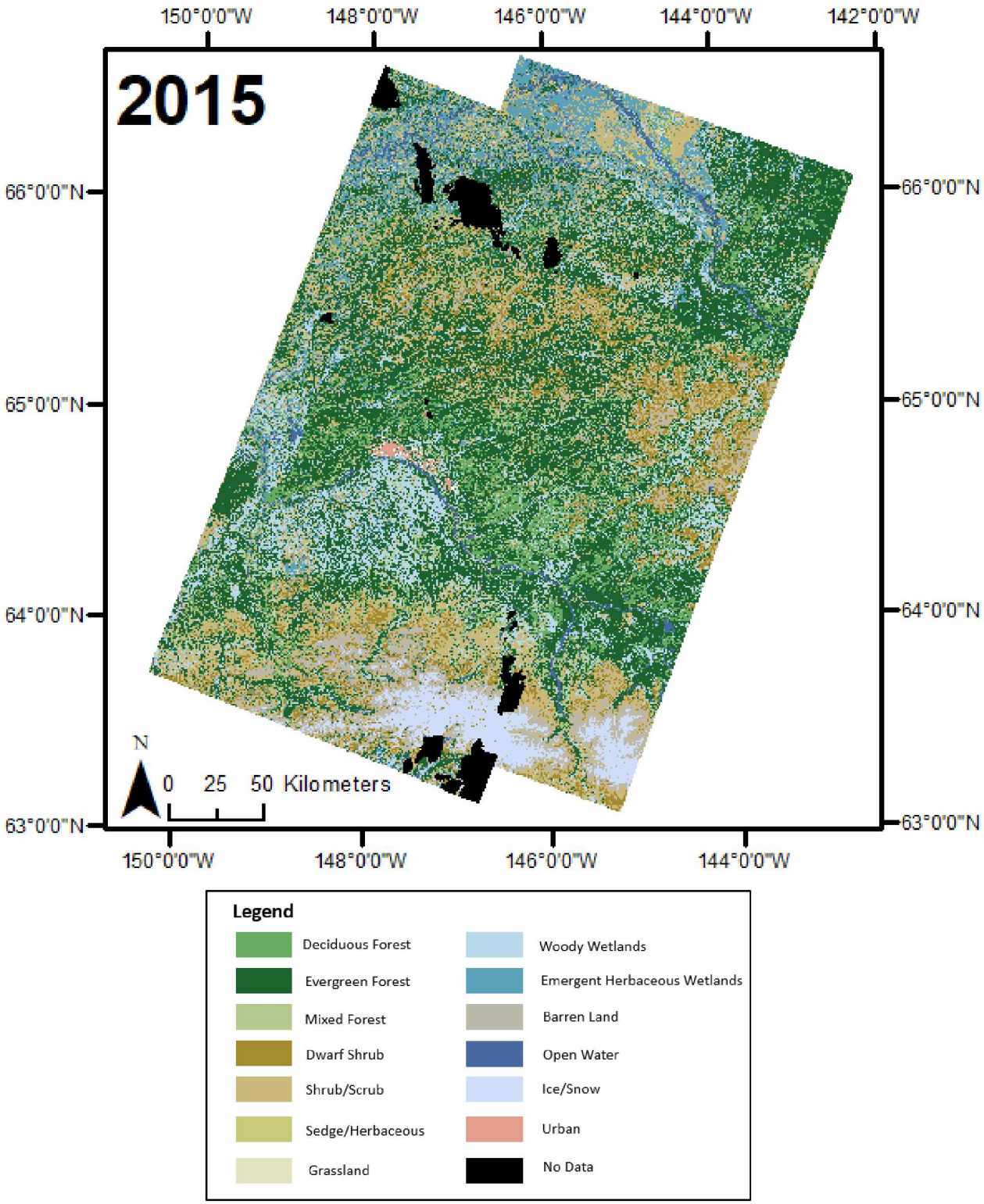

Figure 21. 2015 Vegetation Map.

4.2. Classification Model Performance

An accuracy assessment has not been carried out for these classification maps, because of the unavailability of a separately collected set of ground truth data. What is presented here is a model evaluation using 20% of separately withheld unseen instances of the training data. The model evaluations were carried out before post-processing pixel edits and the placement of the masks. These should only be used to reflect the accuracy of the model, not the classification itself. For a true accuracy assessment of a classified map to be carried out, the training data used to generate the map should be compared to a set of fairly accurate reference data collected separately in the field. The inability to find separately collected ground truth data has prevented us from performing a true accuracy assessment. If an accuracy assessment is carried out using the same training data, any inherent biases would also be extrapolated to the accuracy assessment allowing for potential errors to remain unrecognized and not quantified. For this reason, the statistics provided below only represent how the model itself is preforming in classifying each class, not the actual accuracy of the classes (Congalton, 1991).

The overall model accuracy is calculated by dividing the total number of correctly classified points (diagonal in the error matrix) by the total number of points within the error matrix. As it is named, the overall accuracy gives a general idea of the model's performance, but more detailed calculations are needed to assess each class separately. The producer's accuracy is calculated by dividing the number of correct pixels for each class by the total number of pixels in that class. This accuracy represents the probability of a reference point of that class being classified correctly. It gives the producer of the map an idea about how accurately each class can be classified. The user's accuracy is calculated by dividing the number of correctly classified points by the total number of points classified as that class. This accuracy provides the reliability to the user of the map that each class on the map actually represents that class on the ground. The kappa analysis is computed by running the KHAT statistic (Equation 3). The kappa analysis can be used to determine how much better the results are from the error matrix than random results. A kappa value of 0 means that our results are no better than a random result, while a kappa value

closer to 1 indicates that our results are significantly better than a random result (Congalton, 1991).

$$K = \frac{N \sum_{i=1}^{r} x_{ii} - \sum_{i=1}^{r} (x_{i+} * x_{+i})}{N^2 - \sum_{i=1}^{r} (x_{i+} * x_{+i})}$$

Equation 3. KHAT statistic. N is the total number of observations, r is the number of rows in the matrix, x_{ii} is the number of observations in row i and column i, x_{i+} and x_{+i} are the marginal totals of row i and column i, respectively (From Congalton 1991).

4.2.1. 1985 Classification Model Performance

Table 4. 1985 map northwest and southwest scenes classification model performance in number of pixels

P69 R14 & 15 - September 22nd 1984	a	b	c	d	e	f	g	h	i	j	k	l	Total	P69 R14&15 - September 22nd 1984	User's	Producer's
Deciduous Forest (a)	14212	213	94	0	55	11	0	46	32	6	0	0	14669	Deciduous Forest	96.9%	94.7%
Evergreen Forest (b)	262	28141	138	10	95	4	2	145	47	14	6	0	28864	Evergreen Forest	97.5%	95.0%
Mixed Forest (c)	251	447	3635	6	46	3	0	114	33	4	0	0	4539	Mixed Forest	80.1%	89.8%
Dwarf Shrub (d)	4	25	8	783	41	5	2	5	54	4	0	0	931	Dwarf Shrub	84.1%	89.4%
Shrub/Scrub (e)	141	187	56	28	7097	21	11	49	318	16	10	0	7934	Shrub/Scrub	89.5%	90.7%
Sedge/Herbaceous (f)	12	21	4	5	59	667	3	5	40	5	1	0	822	Sedge/Herbaceous	81.1%	89.8%
Grassland/Herbaceous (g)	4	6	2	7	26	5	350	2	32	0	0	0	434	Grassland/Herbaceous	80.6%	92.1%
Woody Wetlands (h)	42	399	66	3	46	3	3	4832	80	2	6	0	5482	Woody Wetlands	88.1%	90.0%
Emergent Herbaceous Wetlands (i)	52	142	39	31	298	21	6	160	5701	7	3	0	6460	Emergent Herbaceous Wetlands	88.3%	89.6%
Barren Land (j)	20	22	3	3	43	3	3	5	14	816	4	1	937	Barren Land	87.1%	93.0%
Open Water (k)	4	9	3	0	16	0	0	6	10	0	6203	0	6251	Open Water	99.2%	99.5%
Ice/Snow (l)	0	0	0	0	0	0	0	0	0	3	0	6425	6428	Ice/Snow	100.0%	100.0%
Total	15004	29612	4048	876	7822	743	380	5369	6361	877	6233	6426	83751			

Table 5. 1985 map northeast and southeast scenes classification model performance in number of pixels

P68 R14 & 15 - August 1st & 3rd 1985 & 1987	a	b	c	d	e	f	g	h	i	j	k	l	Total	P68 R14 & 15 - August 1st & 3rd 1985 & 1987	User's	Producer's
Deciduous Forest (a)	18251	283	81	5	63	1	0	50	28	0	2	0	18764	Deciduous Forest	97.3%	93.5%
Evergreen Forest (b)	449	24646	146	23	170	7	3	232	112	0	5	0	25793	Evergreen Forest	95.6%	92.3%
Mixed Forest (c)	392	484	1818	11	70	1	1	101	36	0	2	0	2916	Mixed Forest	62.3%	82.7%
Dwarf Shrub (d)	27	54	5	670	110	5	3	18	84	4	1	1	982	Dwarf Shrub	68.2%	81.1%
Shrub/Scrub (e)	236	336	44	66	4263	33	15	101	641	6	4	2	5747	Shrub/Scrub	74.2%	77.5%
Sedge/Herbaceous (f)	7	29	5	7	88	255	5	8	115	0	0	0	519	Sedge/Herbaceous	49.1%	72.9%
Grassland/Herbaceous (g)	1	22	2	3	28	4	172	10	39	2	1	0	284	Grassland/Herbaceous	60.6%	77.5%
Woody Wetlands (h)	81	646	65	9	139	4	9	2411	93	2	5	1	3465	Woody Wetlands	69.6%	79.4%
Emergent Herbaceous Wetlands (i)	73	186	26	27	548	39	14	97	3236	2	2	2	4252	Emergent Herbaceous Wetlands	76.1%	73.4%
Barren Land (j)	6	16	1	5	17	1	0	1	20	444	6	0	517	Barren Land	85.9%	96.5%
Open Water (k)	1	11	4	0	6	0	0	4	7	0	5194	0	5227	Open Water	99.4%	99.5%
Ice/Snow (l)	0	0	0	0	1	0	0	2	0	0	0	9700	9703	Ice/Snow	100.0%	99.9%
Total	19524	26713	2197	826	5503	350	222	3035	4411	460	5222	9706	78169			

The northwest and southwest scenes had an overall accuracy of 94.2% and a kappa index of 0.93. The northeast and southeast scenes had an overall accuracy of 90.9% and a kappa index of 0.89. Some classes are consistent over each scene, and others differed in accuracy. Deciduous and evergreen classified very well with accuracies at or above 92.3%. Mixed forest, dwarf shrub, shrub, woody wetlands and emergent herbaceous wetlands all performed well having accuracies ranging between 80.1-90.7% for the northwest and southwest scenes but performed moderately in the northeast and southeast scenes having ranges between 62.4-82.8%. Grassland and sedge had the fewest ground truth points out of all the classes resulting in wide ranges of accuracy. For the northwest and southwest scenes, the accuracies were between 80.7-92.1%, and ranges of 49.1-77.5% for the northeast and southeast scenes. Grassland and sedge accounted for the least percentage of training data throughout all scenes, and is most likely the reasoning behind the wide ranges of accuracies. Open water and ice/snow performed very well with 99.2% accuracy or above, and barren land also performed well, between 85.9-96.5%.

4.2.2. 1995 Classification Model Performance

Table 6. 1995 map northwest and southwest scenes classification model performance in number of pixels

P69 R14 & 15 - June 22nd 1991	a	b	c	d	e	f	g	h	i	j	k	l	Total	P69 R14 & 15 - June 22nd 1991	User's	Producer's
Deciduous Forest (a)	12914	350	194	2	94	1	2	113	42	6	0	0	13718	Deciduous Forest	94.1%	90.6%
Evergreen Forest (b)	410	23147	302	21	254	12	8	443	192	12	2	0	24803	Evergreen Forest	93.3%	86.6%
Mixed Forest (c)	448	810	2194	12	91	4	2	220	97	6	4	0	3888	Mixed Forest	56.4%	72.2%
Dwarf Shrub (d)	7	53	9	438	79	6	2	22	41	10	4	0	671	Dwarf Shrub	65.3%	76.2%
Shrub/Scrub (e)	250	691	82	42	3767	42	29	235	424	21	11	0	5594	Shrub/Scrub	67.3%	73.9%
Sedge/Herbaceous (f)	19	83	11	2	91	278	5	27	52	1	0	0	569	Sedge/Herbaceous	48.9%	73.0%
Grassland/Herbaceous (g)	15	33	4	3	66	7	195	10	24	2	0	0	359	Grassland/Herbaceous	54.3%	73.6%
Woody Wetlands (h)	71	921	144	14	132	4	8	3087	166	0	4	0	4551	Woody Wetlands	67.8%	69.5%
Emergent Herbaceous Wetlands (i)	100	552	86	24	459	27	11	271	2834	15	12	0	4391	Emergent Herbaceous Wetlands	64.5%	72.3%
Barren Land (j)	17	67	11	17	54	0	3	6	29	248	6	0	458	Barren Land	54.1%	76.1%
Open Water (k)	8	31	3	0	13	0	0	5	18	5	6888	0	6971	Open Water	98.8%	99.4%
Ice/Snow (l)	0	0	0	0	0	0	0	0	0	0	0	2600	2600	Ice/Snow	100.0%	100.0%
Total	14259	26738	3040	575	5100	381	265	4439	3919	326	6931	2600	68573			

Table 7. 1995 map northeast and southeast scenes classification model performance in number of pixels

P68 R14 & 15 - July 14th 1993	a	b	c	d	e	f	g	h	i	j	k	l	Total	P68 R14 & 15 - July 14th 1993	User's	Producer's
Deciduous Forest (a)	17481	219	97	6	42	2	1	52	22	0	1	0	17923	Deciduous Forest	97.5%	94.1%
Evergreen Forest (b)	362	23210	145	9	146	8	4	265	97	2	1	0	24249	Evergreen Forest	95.7%	92.1%
Mixed Forest (c)	420	513	1332	6	49	0	0	140	26	1	1	0	2488	Mixed Forest	53.5%	77.4%
Dwarf Shrub (d)	22	41	8	497	49	2	0	4	27	3	0	0	653	Dwarf Shrub	76.1%	82.4%
Shrub/Scrub (e)	161	344	35	48	3079	16	13	86	349	7	0	2	4140	Shrub/Scrub	74.4%	78.9%
Sedge/Herbaceous (f)	2	35	2	4	46	197	4	8	62	1	1	0	362	Sedge/Herbaceous	54.4%	77.9%
Grassland/Herbaceous (g)	5	14	1	8	19	0	81	2	30	0	0	0	160	Grassland/Herbaceous	50.6%	69.2%
Woody Wetlands (h)	85	597	76	4	106	1	3	2116	105	5	4	1	3103	Woody Wetlands	68.2%	73.9%
Emergent Herbaceous Wetlands (i)	40	203	19	14	349	25	11	189	2283	2	10	0	3145	Emergent Herbaceous Wetlands	72.6%	75.6%
Barren Land (j)	7	21	3	7	12	2	0	1	7	302	1	0	363	Barren Land	83.2%	92.9%
Open Water (k)	0	13	4	0	4	0	0	2	10	2	4986	1	5022	Open Water	99.3%	99.6%
Ice/Snow (l)	0	0	0	0	0	0	0	0	0	0	0	8144	8144	Ice/Snow	100.0%	100.0%
Total	18585	25210	1722	603	3901	253	117	2865	3018	325	5005	8148	69752			

The northwest and southwest scenes had an overall accuracy of 85.4% and a kappa index of 0.82. The northeast and southeast scenes had an overall accuracy of 91.3% and a kappa index of 0.89. The scenes in this map were the closest in their phenology compared to the other years and resulted around the same ranges of accuracies for each class. Deciduous and evergreen forests had accuracies at or above 86.5%, while mixed forest displayed a wide range between 53.5-77.4%. Dwarf shrub and shrub performed moderately, with ranges between 65.3%-82.4%. Woody wetlands and emergent herbaceous wetlands had similar ranges, between 50.6-75.7%; the difficulties of classifying wetlands is further discussed in section 5.2. Sedge and grassland were the two classes that had accuracies that were less than satisfactory, with ranges between 48.9-77.9%. Open water and ice/snow did very well having all accuracies at 98.8% or above. Barren land was close behind, with accuracies between 78.1-91.7%.

4.2.3 2005 Classification Model Performance

Table 8. 2005 map northwest scene classification model performance in number of pixels

P69 R14 - September 3rd 2006	a	b	c	d	e	f	g	h	i	j	k	l	Total	P69 R14 - September 3rd 2006	User's	Producer's
Deciduous Forest (a)	13696	193	95	2	56	2	1	68	29	2	0	0	14144	Deciduous Forest	96.8%	94.7%
Evergreen Forest (b)	288	26046	169	4	99	5	2	163	127	7	3	0	26913	Evergreen Forest	96.8%	93.8%
Mixed Forest (c)	248	486	3053	2	48	4	0	93	34	3	1	0	3972	Mixed Forest	76.9%	87.7%
Dwarf Shrub (d)	6	25	6	472	27	3	0	7	35	3	3	0	587	Dwarf Shrub	80.4%	89.6%
Shrub/Scrub (e)	115	274	41	24	4098	4	7	66	187	28	2	0	4846	Shrub/Scrub	84.6%	89.2%
Sedge/Herbaceous (f)	7	31	6	0	16	314	2	4	19	2	0	0	401	Sedge/Herbaceous	78.3%	91.3%
Grassland/Herbaceous (g)	1	3	0	0	18	1	181	0	26	0	1	0	231	Grassland/Herbaceous	78.4%	88.7%
Woody Wetlands (h)	40	399	73	4	45	4	2	4253	91	1	4	0	4916	Woody Wetlands	86.5%	88.5%
Emergent Herbaceous Wetlands (i)	38	268	32	19	158	6	9	147	3533	10	7	0	4227	Emergent Herbaceous Wetlands	83.6%	86.2%
Barren Land (j)	19	20	5	0	25	1	0	2	13	652	6	1	744	Barren Land	87.6%	92.1%
Open Water (k)	0	18	1	0	4	0	0	2	4	0	6987	0	7016	Open Water	99.6%	99.6%
Ice/Snow (l)	0	0	0	0	0	0	0	0	0	0	0	6111	6111	Ice/Snow	100.0%	100.0%
Total	14458	27763	3481	527	4594	344	204	4805	4098	708	7014	6112	74108			

Table 9. 2005 map northeast and southeast scenes classification model performance in number of pixels

P68 R14&15 - July 18th 2003	a	b	c	d	e	f	g	h	i	j	k	l	Total	P68 R14&15 - July 18th 2003	User's	Producer's
Deciduous Forest (a)	18143	120	59	0	20	1	0	24	12	1	0	0	18380	Deciduous Forest	98.7%	96.8%
Evergreen Forest (b)	192	24665	79	7	39	3	4	49	40	1	1	0	25080	Evergreen Forest	98.3%	96.4%
Mixed Forest (c)	272	216	1795	2	11	0	0	24	13	0	0	0	2333	Mixed Forest	76.9%	90.0%
Dwarf Shrub (d)	5	19	0	713	23	6	1	2	28	1	0	0	798	Dwarf Shrub	89.3%	92.6%
Shrub/Scrub (e)	63	153	15	22	3525	5	4	21	181	8	1	0	3998	Shrub/Scrub	88.2%	92.1%
Sedge/Herbaceous (f)	0	28	2	3	18	283	3	6	36	0	0	0	379	Sedge/Herbaceous	74.7%	89.3%
Grassland/Herbaceous (g)	0	4	0	4	4	1	120	0	7	1	0	0	141	Grassland/Herbaceous	85.1%	82.2%
Woody Wetlands (h)	30	248	26	0	27	2	2	2329	34	0	0	0	2698	Woody Wetlands	86.3%	93.7%
Emergent Herbaceous Wetlands (i)	35	106	19	19	146	14	10	24	3176	4	1	0	3554	Emergent Herbaceous Wetlands	89.4%	89.9%
Barren Land (j)	3	14	0	0	12	2	2	2	4	395	0	4	438	Barren Land	90.2%	95.6%
Open Water (k)	0	5	0	0	2	0	0	4	3	0	5766	0	5780	Open Water	99.8%	99.9%
Ice/Snow (l)	0	0	0	0	0	0	0	0	0	2	0	12309	12311	Ice/Snow	100.0%	100.0%
Total	18743	25578	1995	770	3827	317	146	2485	3534	413	5769	12313	75890			

Table 10. 2005 map southwest scene classification model performance in number of pixels

P69 R15 - August 10th 2003	a	b	c	d	e	f	g	h	i	j	k	l	Total	P69 R15 - August 10th 2003	User's	Producer's
Deciduous Forest (a)	10851	270	156	4	48	0	2	139	27	7	1	0	11505	Deciduous Forest	94.3%	92.0%
Evergreen Forest (b)	298	20345	277	8	100	0	0	481	74	15	2	0	21600	Evergreen Forest	94.2%	89.0%
Mixed Forest (c)	310	804	1804	5	50	4	0	318	38	4	3	0	3340	Mixed Forest	54.0%	69.1%
Dwarf Shrub (d)	8	18	6	205	22	0	0	5	0	4	0	0	268	Dwarf Shrub	76.5%	83.3%
Shrub/Scrub (e)	111	186	55	17	2701	1	0	171	29	7	1	0	3279	Shrub/Scrub	82.4%	88.3%
Sedge/Herbaceous (f)	8	21	15	0	8	51	6	20	0	0	0	0	129	Sedge/Herbaceous	39.5%	82.3%
Grassland/Herbaceous (g)	4	9	1	0	2	0	42	4	3	0	0	0	65	Grassland/Herbaceous	64.6%	72.4%
Woody Wetlands (h)	123	889	215	1	91	1	5	3407	156	6	22	0	4916	Woody Wetlands	69.3%	69.4%
Emergent Herbaceous Wetlands (i)	61	269	71	2	29	4	3	341	643	1	5	0	1429	Emergent Herbaceous Wetlands	45.0%	65.3%
Barren Land (j)	18	25	10	4	8	0	0	13	1	781	2	0	862	Barren Land	90.6%	94.2%
Open Water (k)	1	15	2	0	0	1	0	13	14	4	4411	0	4461	Open Water	98.9%	99.2%
Ice/Snow (l)	0	0	0	0	0	0	0	0	0	0	0	8198	8198	Ice/Snow	100.0%	100.0%
Total	11793	22851	2612	246	3059	62	58	4912	985	829	4447	8198	60052			

The northwest scene had an overall accuracy of 93.6% and a kappa index of 0.92. The northeast and southeast scenes had an overall accuracy of 96.5% and a kappa index of 0.96. The southwest scene had an overall accuracy of 89.0% and a kappa index of 0.86 Deciduous and evergreen performed well throughout all the scenes with having accuracies at 89.0% or above. Mixed forest classified well in the northwest, northeast, and southeast scenes with accuracies ranging from 76.9-90.0%, but the accuracy dropped in the southwest scene with a user's accuracy of 54.0% and producer's accuracy of 69.1%. The two shrub classes performed moderately with accuracies ranging between 76.5-92.6%. Like the mixed forest classes, sedge and grassland had accuracies of between 74.7-91.3% in scenes the northwest, northeast, and southeast scenes but ranged from 39.5% (the lowest accuracy of any class in any scene of this map) to 82.3% in the southwest scene. Wetlands also performed more poorly in the southwest scene, 45.0-69.4%, than in the other scenes, 83.6-93.7%. In all the scenes both the user's and producer's accuracies were at or above 98.9% for open water and ice/snow, and at or above 87.6% for barren land.

4.2.4. *2015* Classification *Model Performance*

Table 11. 2015 northwest and southwest scenes classification model performance in number of pixels

P69 R14&15 - July 13th 2013	a	b	c	d	e	f	g	h	i	j	k	l	Total	P69 R14&15 - July 13th 2013	User's	Producer's
Deciduous Forest (a)	9908	276	204	6	83	0	2	121	60	1	0	0	10661	Deciduous Forest	92.9%	89.9%
Evergreen Forest (b)	393	13803	414	26	311	9	7	559	235	5	7	0	15769	Evergreen Forest	87.5%	81.6%
Mixed Forest (c)	386	809	2282	6	129	3	4	254	97	9	0	0	3979	Mixed Forest	57.4%	67.7%
Dwarf Shrub (d)	9	50	11	549	94	1	1	16	50	13	3	0	797	Dwarf Shrub	68.9%	77.1%
Shrub/Scrub (e)	150	525	144	65	3345	26	6	258	362	26	7	0	4914	Shrub/Scrub	68.1%	72.0%
Sedge/Herbaceous (f)	3	68	9	2	70	164	1	33	40	1	0	0	391	Sedge/Herbaceous	41.9%	75.2%
Grassland/Herbaceous (g)	1	5	3	0	1	0	24	3	2	0	0	0	39	Grassland/Herbaceous	61.5%	38.1%
Woody Wetlands (h)	84	857	179	9	190	6	2	2818	176	0	6	0	4327	Woody Wetlands	65.1%	64.9%
Emergent Herbaceous Wetlands (i)	68	453	110	31	350	7	16	259	2093	21	16	0	3424	Emergent Herbaceous Wetlands	61.1%	65.7%
Barren Land (j)	10	64	12	16	50	0	0	8	44	397	4	1	606	Barren Land	65.5%	83.6%
Open Water (k)	4	12	3	2	25	2	0	13	27	2	5210	0	5300	Open Water	98.3%	99.2%
Ice/Snow (l)	0	0	0	0	0	0	0	0	0	0	0	6157	6157	Ice/Snow	100.0%	100.0%
Total	11016	16922	3371	712	4648	218	63	4342	3186	475	5253	6158	56364			

Table 12. 2015 map northeast and southeast scenes classification model performance in number of pixels

P68 R14&15 - June 18th 2013	a	b	c	d	e	f	g	h	i	j	k	l	Total	P68 R14&15 - June 18th 2013	User's	Producer's
Deciduous Forest (a)	14917	126	62	2	17	2	0	24	9	6	0	0	15165	Deciduous Forest	98.4%	96.7%
Evergreen Forest (b)	149	17442	113	8	50	1	0	64	29	1	2	0	17859	Evergreen Forest	97.7%	95.8%
Mixed Forest (c)	262	266	1985	0	14	0	0	29	12	0	0	0	2568	Mixed Forest	77.3%	89.3%
Dwarf Shrub (d)	1	4	1	988	27	1	0	3	21	1	0	0	1047	Dwarf Shrub	94.4%	94.7%
Shrub/Scrub (e)	51	95	10	29	2813	0	1	34	101	4	3	0	3141	Shrub/Scrub	89.6%	92.6%
Sedge/Herbaceous (f)	0	5	0	0	0	38	0	0	2	0	0	0	45	Sedge/Herbaceous	84.4%	84.4%
Grassland/Herbaceous (g)	2	5	0	0	0	0	120	3	3	0	0	0	133	Grassland/Herbaceous	90.2%	96.8%
Woody Wetlands (h)	23	206	41	4	27	0	0	2504	26	1	9	0	2841	Woody Wetlands	88.1%	92.4%
Emergent Herbaceous Wetlands (i)	17	59	9	7	81	3	3	37	1842	4	4	0	2066	Emergent Herbaceous Wetlands	89.2%	90.0%
Barren Land (j)	5	7	2	5	7	0	0	3	2	500	3	0	534	Barren Land	93.6%	96.5%
Open Water (k)	0	1	0	0	1	0	0	8	0	1	5583	0	5594	Open Water	99.8%	99.6%
Ice/Snow (l)	0	0	0	0	0	0	0	0	0	0	0	4912	4912	Ice/Snow	100.0%	100.0%
Total	15427	18216	2223	1043	3037	45	124	2709	2047	518	5604	4912	55905			

The northwest and southwest scenes had an overall accuracy of 82.9% and a kappa index of 0.80. The northeast and southeast scenes had an overall accuracy of 96.0% and a kappa index of 0.95. Classes in the northwest and southwest scenes had an overall lower accuracy compared to the same classes in the northeast and southeast scenes. Deciduous and evergreen performed well with accuracies at 81.6% or above. Dwarf shrub and shrub followed, with accuracies ranging between 68.1-77.1% in the northwest and southwest scenes, and ranges of 89.6-94.7% in the northeast and southeast scenes. Classes mixed forest, woody wetlands, and emergent herbaceous wetlands all performed moderately, with accuracy ranges between 57.4-67.7% for the northwest and southwest scenes, and 77.3-92.4% in the northeast and southeast scenes. Sedge and grassland, once again, had the lowest and widest spread of accuracy results, ranging between 38.1-96.8%. Open water and ice snow continued to perform very well, at or above 98.3%, and barren land ranging between 65.5-96.5%.

4.3. Vegetation Classification Map Overall Weighted Accuracy

An overall weighted accuracy is displayed below for each map. This accuracy was calculated by weighting the overall accuracy for each scene by the percentage of area each scene contributed to the entire map, dictated by the amount of cloud cover in each scene, with least cloudy scenes being displayed in front.

Table 13. Overall weighted accuracy for 1985 vegetation map

1985 Map			
Scenes	**Area Percentage (%)**	**Overall Accuracy (%)**	**Weighted Accuracy (%)**
WRS P69 R14 & 15	69.4	94.2	**93.2**
WRS P68 R14 & 15	30.6	90.9	

Table 14. Overall weighted accuracy for 1995 vegetation map

1995 Map			
Scenes	**Area Percentage (%)**	**Overall Accuracy (%)**	**Weighted Accuracy (%)**
WRS P69 R14 & 15	47.5	85.4	**88.4**
WRS P68 R14	14.5	91.3	
WRS P68 R15	37.9	91.3	

Table 15. Overall weighted accuracy for 2005 vegetation map

2005 Map			
Scenes	**Area Percentage (%)**	**Overall Accuracy (%)**	**Weighted Accuracy (%)**
WRS P69 R14	12.2	93.6	**93.3**
WRS P68 R14 & 15	50.5	96.5	
WRS P69 R15	37.3	89.0	

Table 16. Overall weighted accuracy for 2015 vegetation map

2015 Map			
Scenes	**Percent Area (%)**	**Overall Accuracy (%)**	**Weighted Accuracy (%)**
WRS P69 R14 & 15	69.6	82.9	**86.9**
WRS P68 R14 & 15	30.4	96.0	

4.4. Distribution of Vegetation by Class

The following graphs display the percentage of pixels for each vegetation class. The pixels from the masked areas were extracted and subtracted from the total pixels in the raster. Therefore, pixels from the urban and no data mask have been removed and are not accounted for in the percentage.

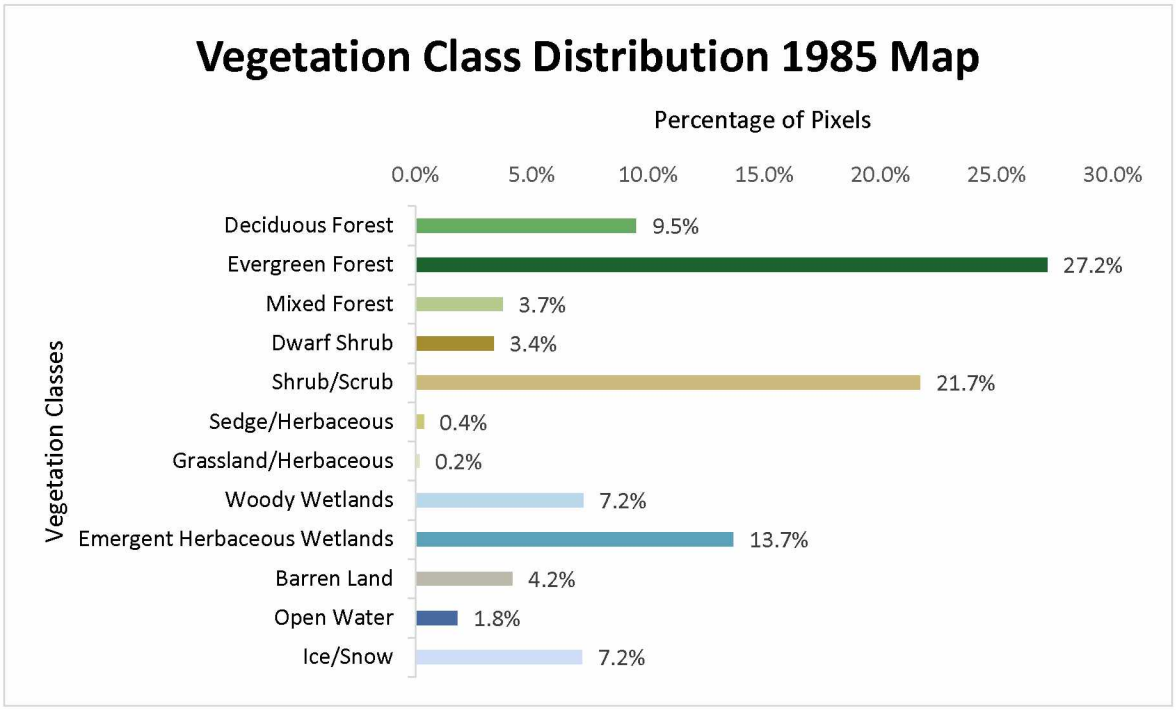

Figure 22. Vegetation class distribution for 1985

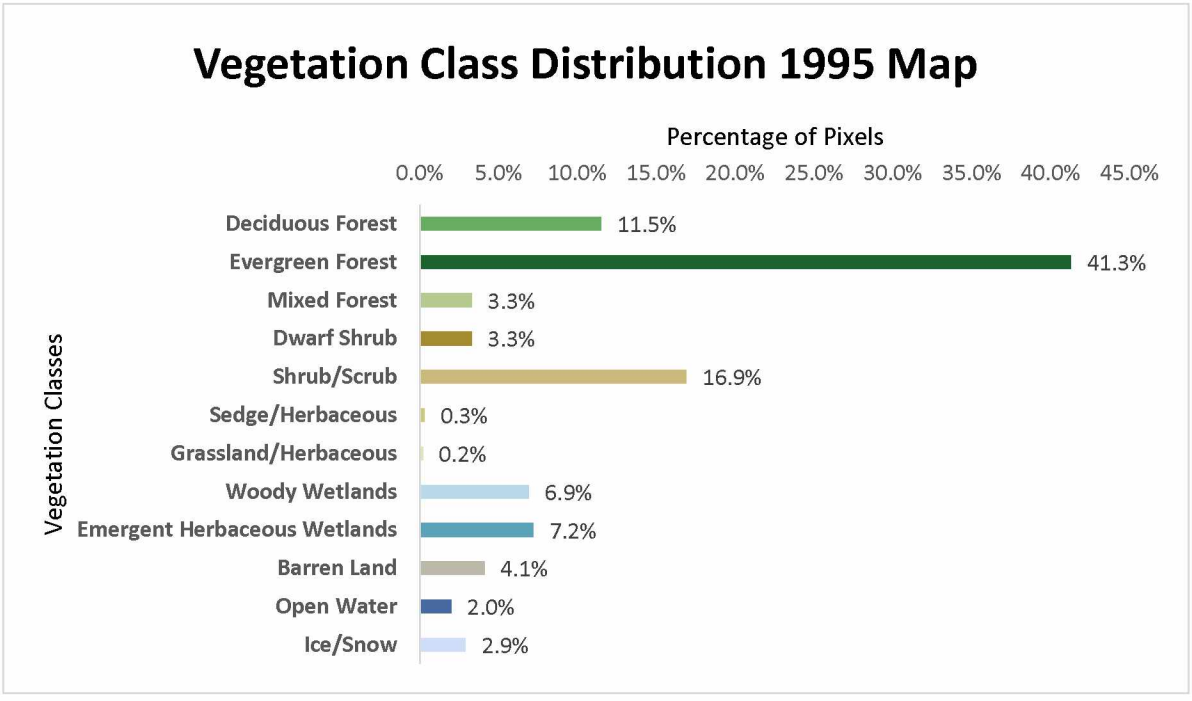

Figure 23. Vegetation class distribution for 1995

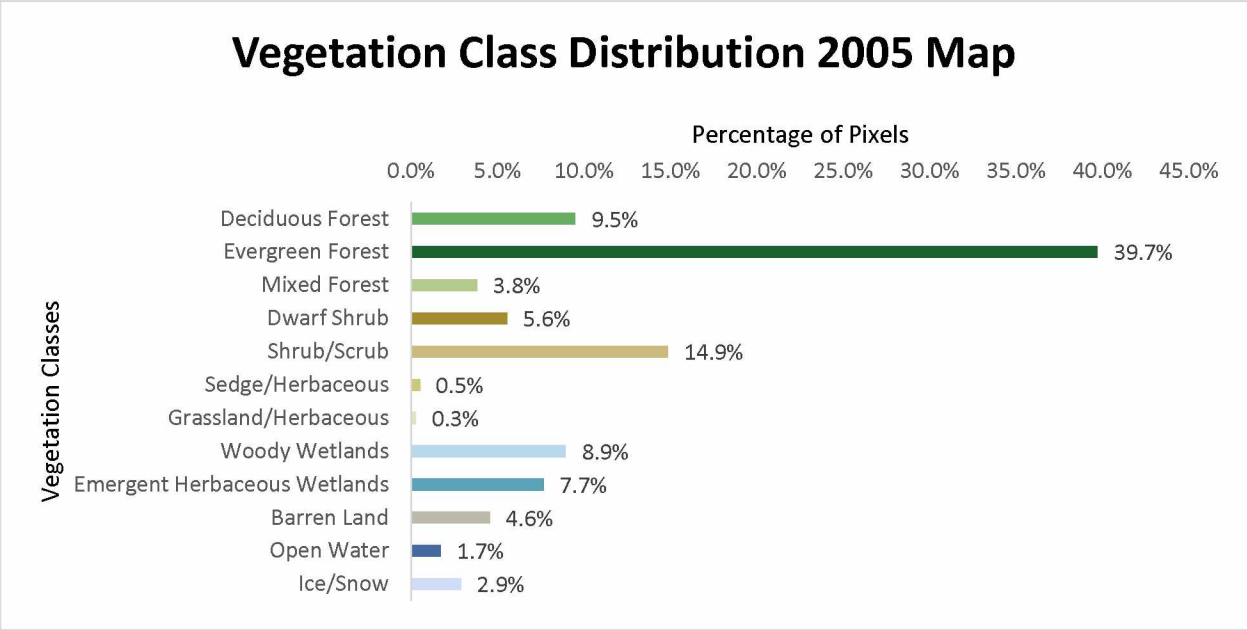

Figure 24. Vegetation class distribution for 2005

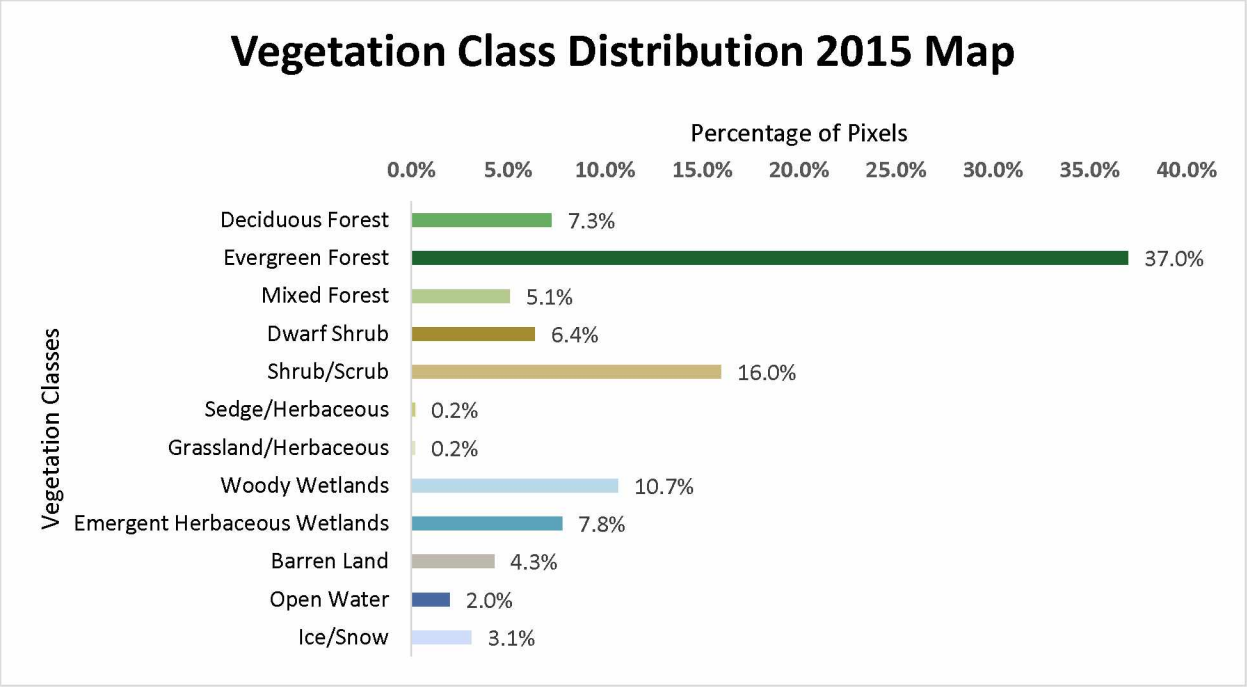

Figure 25. Vegetation class distribution for 2015

4.5. Vegetation Cross-tabulation

The following tables are post classification cross-tabulated area tables, with pixels from the urban and no data mask, and in some tables pixels from fire scars, not accounted for in the percentage. Areas of no change are along the diagonal, while the total percentage of the area of each vegetation class can be found in the last column and along the last row for the two different years. Tables 17, 18, and 19 show the vegetation change between years 1985-1995, 1995-2005, and 2005-2015, respectively. Table 20 shows the vegetation change between the years 1985 and 2015, and table 21 shows the vegetation change between 1995 and 2015. Table 22 shows the vegetation change between the years of 1985 and 2015 but only the southeast and southwest scenes. Tables 23 and 24 show the vegetation change for the same periods of time, but along with the clouds being masked, the fire scars from the years 1980-2018 were also masked.

Table 17. Cross-tabulation between 1985-1995 vegetation maps in percent area.

		TO:												
	Area in %	**Vegetation map 1995**												
	FROM:	a	b	c	d	e	f	g	h	i	j	k	l	**1985 Total**
Vegetation map 1985	Deciduous (a)	4.8	2.2	0.5	0.4	1.0	0.0	0.0	0.2	0.1	0.1	0.1	0.1	9.5
	Evergreen (b)	2.2	19.1	1.2	0.3	1.8	0.0	0.0	1.5	0.6	0.2	0.2	0.2	27.3
	Mixed Forest (c)	0.6	1.6	0.5	0.1	0.4	0.0	0.0	0.4	0.1	0.1	0.0	0.0	3.8
	Dwarf Shrub (d)	0.3	0.6	0.1	0.7	1.1	0.0	0.0	0.1	0.1	0.3	0.0	0.1	3.4
	Shrub (e)	1.3	7.5	0.4	1.0	6.7	0.1	0.0	0.9	3.1	0.5	0.2	0.1	21.7
	Sedge (f)	0.0	0.1	0.0	0.0	0.1	0.0	0.0	0.0	0.1	0.0	0.0	0.0	0.4
	Grassland (g)	0.0	0.1	0.0	0.0	0.0	0.0	0.0	0.0	0.0	0.0	0.0	0.0	0.2
	Woody Wetlands (h)	0.2	2.7	0.3	0.0	0.7	0.0	0.0	2.5	0.3	0.1	0.2	0.1	7.2
	Emergent Herbaceous Wetlands (i)	0.6	4.9	0.3	0.2	3.1	0.1	0.0	0.9	3.0	0.1	0.2	0.0	13.4
	Barren Land (j)	0.2	0.5	0.1	0.5	0.9	0.0	0.0	0.2	0.0	1.5	0.1	0.2	4.2
	Open Water (k)	0.0	0.1	0.0	0.0	0.1	0.0	0.0	0.1	0.1	0.1	1.2	0.0	1.7
	Ice/snow (l)	0.1	0.4	0.0	0.5	1.1	0.0	0.0	0.0	0.0	2.0	0.0	3.0	7.3
	1995 Total:	10.3	39.8	3.4	3.8	16.9	0.3	0.2	6.9	7.5	5.0	2.3	3.8	

Table 18. Cross-tabulation between 1995-2005 vegetation maps in percent area.

	TO:												
	Area in %	**Vegetation map 2005**												
	FROM:	a	b	c	d	e	f	g	h	i	j	k	l	**1995 Total**
Vegetation map 1995	Deciduous (a)	5.3	2.4	0.7	0.6	0.9	0.0	0.0	0.4	0.3	0.1	0.0	0.0	10.7
	Evergreen (b)	2.1	26.2	1.5	0.9	3.6	0.2	0.1	3.6	2.0	0.3	0.1	0.0	40.6
	Mixed Forest (c)	0.5	1.4	0.5	0.1	0.3	0.0	0.0	0.4	0.1	0.0	0.0	0.0	3.4
	Dwarf Shrub (d)	0.2	0.5	0.1	1.3	1.1	0.0	0.0	0.1	0.1	0.4	0.0	0.0	3.8
	Shrub (e)	0.9	4.0	0.5	1.5	5.6	0.1	0.1	1.1	2.0	0.5	0.1	0.1	16.3
	Sedge (f)	0.0	0.1	0.0	0.0	0.1	0.0	0.0	0.0	0.1	0.0	0.0	0.0	0.3
	Grassland (g)	0.0	0.1	0.0	0.0	0.0	0.0	0.0	0.0	0.0	0.0	0.0	0.0	0.2
	Woody Wetlands (h)	0.2	2.3	0.3	0.1	0.6	0.0	0.0	2.5	0.5	0.1	0.1	0.0	6.6
	Emergent Herbaceous Wetlands (i)	0.2	1.8	0.2	0.1	1.8	0.1	0.1	0.5	2.2	0.0	0.1	0.0	7.1
	Barren Land (j)	0.1	0.4	0.0	0.5	0.5	0.0	0.0	0.1	0.1	2.4	0.1	0.4	4.6
	Open Water (k)	0.0	0.3	0.0	0.1	0.1	0.0	0.0	0.2	0.1	0.1	1.3	0.0	2.4
	Ice/snow (l)	0.1	0.4	0.0	0.3	0.2	0.0	0.0	0.1	0.0	0.5	0.0	2.3	3.9
2005 Total:		9.6	40.0	3.9	5.5	14.8	0.5	0.3	9.0	7.5	4.5	1.7	2.9	

Table 19. Cross-tabulation between 2005-2015 vegetation maps in percent area.

	TO:												
	Area in %	**Vegetation map 2015**												
	FROM:	a	b	c	d	e	f	g	h	i	j	k	l	**2005 Total**
Vegetation map 2005	Deciduous (a)	4.2	2.2	1.0	0.3	1.2	0.0	0.0	0.3	0.3	0.0	0.0	0.0	9.6
	Evergreen (b)	2.0	24.8	2.3	0.8	3.3	0.0	0.0	4.7	1.5	0.2	0.1	0.0	39.9
	Mixed Forest (c)	0.4	1.5	0.7	0.1	0.4	0.0	0.0	0.4	0.2	0.0	0.0	0.0	3.8
	Dwarf Shrub (d)	0.0	0.5	0.1	2.5	1.6	0.0	0.0	0.1	0.2	0.4	0.0	0.1	5.4
	Shrub (e)	0.4	3.4	0.4	1.5	5.5	0.0	0.0	1.1	1.8	0.4	0.1	0.1	14.9
	Sedge (f)	0.0	0.1	0.0	0.0	0.1	0.0	0.0	0.1	0.1	0.0	0.0	0.0	0.5
	Grassland (g)	0.0	0.0	0.0	0.0	0.1	0.0	0.0	0.0	0.1	0.0	0.0	0.0	0.3
	Woody Wetlands (h)	0.3	2.9	0.4	0.2	1.1	0.0	0.0	3.3	0.6	0.1	0.1	0.0	9.1
	Emergent Herbaceous Wetlands (i)	0.2	2.1	0.2	0.1	1.4	0.0	0.1	0.8	2.6	0.0	0.1	0.0	7.7
	Barren Land (j)	0.0	0.2	0.0	0.5	0.5	0.0	0.0	0.0	0.1	2.3	0.1	0.6	4.3
	Open Water (k)	0.0	0.1	0.0	0.0	0.1	0.0	0.0	0.1	0.1	0.0	1.3	0.0	1.7
	Ice/snow (l)	0.0	0.0	0.0	0.1	0.2	0.0	0.0	0.0	0.0	0.4	0.0	2.2	2.8
2015 Total:		7.6	37.9	5.3	6.1	15.5	0.2	0.2	10.9	7.4	3.9	1.9	3.0	

Table 20. Cross-tabulation between 1985-2015 vegetation maps in percent area.

	TO:												
	Area in %	**Vegetation map 2015**											
	FROM:	a	b	c	d	e	f	g	h	i	j	k	l	**1985 Total**
Vegetation map 1985	Deciduous (a)	3.5	2.5	0.9	0.6	1.4	0.0	0.0	0.4	0.2	0.1	0.0	0.0	9.6
	Evergreen (b)	1.6	17.0	1.9	0.7	2.0	0.0	0.0	3.2	0.7	0.1	0.1	0.0	27.5
	Mixed Forest (c)	0.4	1.6	0.6	0.1	0.4	0.0	0.0	0.5	0.1	0.0	0.0	0.0	3.8
	Dwarf Shrub (d)	0.1	0.5	0.1	1.0	1.1	0.0	0.0	0.1	0.1	0.3	0.0	0.0	3.3
	Shrub (e)	0.9	7.7	0.8	1.3	5.6	0.1	0.1	1.7	3.1	0.3	0.1	0.0	21.7
	Sedge (f)	0.0	0.1	0.0	0.0	0.1	0.0	0.0	0.0	0.1	0.0	0.0	0.0	0.4
	Grassland (g)	0.0	0.1	0.0	0.0	0.0	0.0	0.0	0.0	0.0	0.0	0.0	0.0	0.2
	Woody Wetlands (h)	0.3	2.2	0.3	0.1	0.9	0.0	0.0	2.8	0.5	0.1	0.1	0.0	7.3
	Emergent Herbaceous Wetlands (i)	0.5	5.1	0.5	0.2	2.6	0.1	0.1	1.5	2.8	0.1	0.2	0.0	13.5
	Barren Land (j)	0.1	0.5	0.1	0.7	0.9	0.0	0.0	0.1	0.1	1.4	0.2	0.1	4.1
	Open Water (k)	0.0	0.2	0.0	0.0	0.1	0.0	0.0	0.1	0.1	0.1	1.2	0.0	1.8
	Ice/snow (l)	0.0	0.2	0.0	0.9	0.7	0.0	0.0	0.1	0.1	1.8	0.0	3.1	7.0
	2015 Total:	7.3	37.6	5.2	5.6	15.8	0.2	0.2	10.6	7.9	4.3	2.0	3.3	

Table 21. Cross-tabulation between 1995-2015 vegetation maps in percent area.

	TO:												
	Area in %	**Vegetation map 2015**											
	FROM:	a	b	c	d	e	f	g	h	i	j	k	l	**1995 Total**
Vegetation map 1995	Deciduous (a)	4.5	2.7	1.2	0.6	1.7	0.0	0.0	0.5	0.3	0.1	0.0	0.0	11.6
	Evergreen (b)	1.9	25.2	2.3	1.0	3.8	0.1	0.0	4.9	1.7	0.3	0.1	0.0	41.5
	Mixed Forest (c)	0.4	1.3	0.7	0.1	0.3	0.0	0.0	0.3	0.2	0.0	0.0	0.0	3.4
	Dwarf Shrub (d)	0.0	0.3	0.0	1.4	1.1	0.0	0.0	0.1	0.1	0.3	0.0	0.0	3.3
	Shrub (e)	0.5	4.0	0.6	2.0	5.7	0.1	0.0	1.3	2.1	0.3	0.1	0.0	16.7
	Sedge (f)	0.0	0.1	0.0	0.0	0.1	0.0	0.0	0.0	0.1	0.0	0.0	0.0	0.3
	Grassland (g)	0.0	0.1	0.0	0.0	0.0	0.0	0.0	0.0	0.0	0.0	0.0	0.0	0.2
	Woody Wetlands (h)	0.2	2.0	0.3	0.1	0.9	0.0	0.0	2.7	0.5	0.1	0.1	0.0	7.0
	Emergent Herbaceous Wetlands (i)	0.2	2.1	0.2	0.1	1.4	0.0	0.0	0.8	2.1	0.0	0.1	0.0	7.1
	Barren Land (j)	0.0	0.1	0.0	0.3	0.3	0.0	0.0	0.0	0.1	2.4	0.1	0.6	4.0
	Open Water (k)	0.0	0.2	0.0	0.0	0.1	0.0	0.0	0.1	0.1	0.1	1.4	0.0	2.0
	Ice/snow (l)	0.0	0.0	0.0	0.0	0.0	0.0	0.0	0.0	0.0	0.3	0.0	2.5	2.9
	2015 Total:	7.8	38.0	5.3	5.7	15.5	0.2	0.2	10.9	7.4	3.9	1.9	3.2	

Table 22. Cross-tabulation in percent area between the southeast and southwest corners of the 1985-2015 vegetation maps.

	TO:												
	Area in %	**Vegetation map 2015**											
	FROM:	a	b	c	d	e	f	g	h	i	j	k	l	**1985 Total**
Vegetation map 1985	Deciduous (a)	5.2	3.0	1.2	0.5	1.6	0.0	0.0	0.7	0.1	0.1	0.0	0.0	12.4
	Evergreen (b)	2.4	23.0	2.6	0.7	2.3	0.0	0.0	4.8	0.8	0.2	0.1	0.0	36.8
	Mixed Forest (c)	0.5	2.0	0.8	0.1	0.4	0.0	0.0	0.9	0.2	0.0	0.0	0.0	5.0
	Dwarf Shrub (d)	0.1	0.6	0.1	1.1	1.5	0.0	0.0	0.2	0.0	0.4	0.0	0.0	4.1
	Shrub (e)	0.4	1.5	0.4	0.7	2.8	0.0	0.0	0.9	0.2	0.2	0.0	0.0	7.2
	Sedge (f)	0.0	0.0	0.0	0.0	0.0	0.0	0.0	0.0	0.0	0.0	0.0	0.0	0.0
	Grassland (g)	0.0	0.0	0.0	0.0	0.0	0.0	0.0	0.0	0.0	0.0	0.0	0.0	0.1
	Woody Wetlands (h)	0.4	3.3	0.5	0.2	1.4	0.0	0.0	4.7	0.7	0.2	0.2	0.0	11.6
	Emergent Herbaceous Wetlands (i)	0.1	0.7	0.2	0.0	0.4	0.0	0.0	0.8	0.3	0.0	0.1	0.0	2.6
	Barren Land (j)	0.1	0.7	0.1	1.0	1.4	0.0	0.0	0.2	0.2	2.3	0.3	0.2	6.4
	Open Water (k)	0.0	0.2	0.0	0.0	0.0	0.0	0.0	0.1	0.0	0.1	0.9	0.0	1.3
	Ice/snow (l)	0.0	0.3	0.0	1.5	1.3	0.0	0.0	0.1	0.2	3.3	0.0	5.5	12.3
	2015 Total:	9.4	35.5	5.9	5.9	13.0	0.1	0.1	13.2	2.8	6.7	1.6	5.9	

Table 23. Cross-tabulation in percent area between 1985-2015 vegetation maps, with fire scars masked.

	TO:												
	Area in %	**Vegetation map 2015**											
	FROM:	a	b	c	d	e	f	g	h	i	j	k	l	**1985 Total**
Vegetation map 1985	Deciduous (a)	4.2	2.6	1.0	0.6	1.7	0.0	0.0	0.5	0.1	0.1	0.0	0.0	10.9
	Evergreen (b)	1.7	17.2	2.2	0.6	1.7	0.0	0.0	3.1	0.6	0.1	0.1	0.0	27.5
	Mixed Forest (c)	0.4	1.7	0.7	0.1	0.4	0.0	0.0	0.4	0.1	0.0	0.0	0.0	4.0
	Dwarf Shrub (d)	0.1	0.6	0.1	1.3	1.5	0.0	0.0	0.1	0.1	0.4	0.0	0.0	4.3
	Shrub (e)	0.6	5.6	0.8	1.4	5.2	0.1	0.0	1.2	2.6	0.3	0.2	0.0	18.0
	Sedge (f)	0.0	0.1	0.0	0.0	0.1	0.0	0.0	0.0	0.0	0.0	0.0	0.0	0.3
	Grassland (g)	0.0	0.0	0.0	0.0	0.0	0.0	0.0	0.0	0.0	0.0	0.0	0.0	0.1
	Woody Wetlands (h)	0.3	2.1	0.3	0.1	0.6	0.0	0.0	2.4	0.4	0.1	0.2	0.0	6.6
	Emergent Herbaceous Wetlands (i)	0.3	3.6	0.4	0.2	2.0	0.1	0.0	1.0	2.6	0.1	0.2	0.0	10.4
	Barren Land (j)	0.1	0.6	0.1	0.9	1.2	0.0	0.0	0.1	0.2	2.0	0.2	0.2	5.7
	Open Water (k)	0.0	0.2	0.0	0.0	0.1	0.0	0.0	0.1	0.1	0.1	1.6	0.0	2.2
	Ice/snow (l)	0.0	0.3	0.0	1.3	1.0	0.0	0.0	0.1	0.2	2.7	0.0	4.5	10.0
	2015 Total:	7.7	34.7	5.7	6.5	15.6	0.2	0.2	9.2	7.1	6.0	2.5	4.8	

Table 24. Cross-tabulation in percent area between 1995-2015 vegetation maps, with fire scars masked.

	TO:												
	Area in %	**Vegetation map 2015**											
	FROM:	a	b	c	d	e	f	g	h	i	j	k	l	**1995 Total**
Vegetation map 1995	Deciduous (a)	5.4	2.8	1.4	0.7	2.0	0.0	0.0	0.5	0.3	0.1	0.0	0.0	13.2
	Evergreen (b)	1.6	23.7	2.4	0.9	2.8	0.0	0.0	4.4	1.4	0.3	0.2	0.0	37.8
	Mixed Forest (c)	0.4	1.3	0.8	0.1	0.3	0.0	0.0	0.3	0.2	0.0	0.0	0.0	3.5
	Dwarf Shrub (d)	0.0	0.3	0.1	1.9	1.4	0.0	0.0	0.1	0.1	0.4	0.0	0.0	4.3
	Shrub (e)	0.3	3.3	0.6	2.5	6.2	0.0	0.0	1.1	1.8	0.5	0.1	0.0	16.5
	Sedge (f)	0.0	0.1	0.0	0.0	0.1	0.0	0.0	0.0	0.0	0.0	0.0	0.0	0.2
	Grassland (g)	0.0	0.0	0.0	0.0	0.1	0.0	0.0	0.0	0.0	0.0	0.0	0.0	0.2
	Woody Wetlands (h)	0.2	1.8	0.3	0.1	0.6	0.0	0.0	2.2	0.4	0.1	0.2	0.0	5.9
	Emergent Herbaceous Wetlands (i)	0.1	1.4	0.2	0.1	1.2	0.0	0.0	0.5	2.1	0.0	0.1	0.0	5.9
	Barren Land (j)	0.0	0.2	0.0	0.5	0.5	0.0	0.0	0.0	0.1	3.6	0.1	0.9	5.8
	Open Water (k)	0.0	0.2	0.0	0.0	0.1	0.0	0.0	0.1	0.1	0.1	1.8	0.0	2.5
	Ice/snow (l)	0.0	0.0	0.0	0.0	0.1	0.0	0.0	0.0	0.0	0.4	0.0	3.7	4.2
	2015 Total:	8.2	35.2	5.8	6.9	15.2	0.2	0.2	9.4	6.5	5.4	2.5	4.7	

5. DISCUSSION

This chapter briefly discusses the advantages in using remote sensing imagery for vegetation classification, the challenges and uncertainties in using multitemporal images for remote sensing vegetation classification, a more in-depth analysis of how the classification model performed for each vegetation class, and a cross tabulated area analysis for investigating changes in vegetation over time.

5.1. Limitations in Using Multitemporal Datasets for Vegetation Classification

Before the use of remote sensing, field surveys, map interpretation, literature reviews, and ancillary data analysis were used to map vegetation. These methods are expensive, date restrictive, and time consuming compared to the practicality and economical means remote sensing techniques introduce. The availability of free Landsat data has made it significantly less difficult to conduct repeatable and cost-efficient vegetation studies, especially covering large or more remote areas. Using remote sensing imagery, one can continually go back and study how the land cover looked in the past and use this information to study how the land cover has been changing and investigate what possible changes may lie ahead (Song and Woodcock, 2003; Xie et al., 2008). Although remote sensing has opened many doors for mapping and detecting vegetation change, errors in mapping vegetation using multitemporal data sets can be introduced from a variety of different aspects and are described in more detail below. Any one, or a combination of, these aspects can introduce differences between scenes collected on different days, months, and years, and possibly cause differences in the classification accuracy between different scenes used in this study.

One of largest obstacles for optical remote sensing is the noise produced by the atmosphere. Satellites collect electromagnetic radiation signals in the solar spectrum where gases (water vapor and ozone) and aerosols cause scattering and absorption and interfere with the

electromagnetic radiation when traveling through Earth's atmosphere from the Earth's surface back to the sensor on the satellite. In some cases, atmospheric corrections are not necessary for vegetation classification; for instance, classification using a single image, or in cases where the training data is derived directly from the image being classified (Song et al., 2001). In this study, not only are multitemporal images being used, but also combinations of training data sets collected over several years, so atmospheric calibration was necessary. The Landsat Surface Reflectance products used in this study underwent atmospheric calibration (carried out by the U.S. Geological Survey Earth Resources Observation and Science Center) to correct for these modifications. A radiative transfer code, 6S (Vermote et al., 1997), was used to correct for scattering/absorption from water vapor and ozone. Total Ozone Mapping Spectrometer aboard Earth Probe platforms or NOAA's Tiros Operational Vertical Sounder was used to get ozone data and column water vapor data was collected from NOAA National Centers for Environmental Prediction to correct to ground truth surface reflectance. (Masek et al., 2006; Song and Woodcock 2003). The dark, dense vegetation method (Kaufman et al., 1997) is used to correct for aerosols (Masek et al., 2006). These correction methods are called full absolute correction, and although one would think images would be more spectrally similar after they have all individually undergone this atmospheric correction, it has been found by Schroeder et al. (2006) and Song et al. (2001) that absolute correction methods make images less spectrally similar to one another. Schroeder et al. (2006) suggested a method referred to as absolute-normalization, in which one image is atmospherically corrected, and then all other images are normalized to this reference image to increase the surface reflectance among images. This normalization processes yields an improved temporal common scale (Schroeder et al., 2006). In addition to this, the USGS reported that in areas with snow covered regions, extensive cloud contamination, low sun angles, and/or areas above 65° latitude (all of which are found in this study) the efficacy of the surface reflectance corrections are likely to be reduced due to adverse atmospheric conditions (USGS, 2018).

Another possible source of error is topography. When correcting for atmospheric noise, it is generally assumed that the landscape is flat. When the topography is flat, sensors aboard

satellites measure the radiances from the vegetation, which is presumed to have a uniform effect. When there are mountainous regions, the geometry between the sun, target orientation, and sensor varies from pixel to pixel (Proy et al., 1989). This alters the viewing angle geometry and introduces a change of direct solar radiation between pixels on slopes, meaning pixels on slopes may appear brighter as they have sent more information back to the satellite compared to pixels in valleys which appear darker, even if they are of the same vegetation type (Riano et al., 2003). In this study, topographic normalization of the data was not carried out. However, we used DEM and DEM derivatives in our classification models that accounted for some of the topographic influences. But, it has been shown that applying radiometric correction (both atmospheric and topographic) will enhance the final reflectance values resulting in better classification results (Gens and Cristobal, 2016; Pons et al., 2014).

Phenology can introduce error when using multitemporal remote sensing images. Angles of illumination change throughout the year with solar zenith decreasing before the summer solstice and increasing afterwards. Vegetation reacts to these changes with many plants growing and flowering at distinct seasonal peaks, and this therefore affects the spectral reflectance observed at that time (Hobbs, 1990). If used correctly (i.e. images with the same phenology are compared, or images are acquired at certain times that specifically highlight certain traits of vegetation), phenology can be used to increase vegetation classification accuracy (Dymond et al., 2002; Son et al., 2013; Xie et al., 2008); but this can be difficult if an area is more often than not under cloud cover and clear images are scarce, preventing from finding images within the same phenology. If cloud free images are not available within the same season, and one is comparing or detecting change from images from different years and months, phenology can become a source of noise and confusion (Coppin et al., 2002; Sexton et al., 2013; Song and Woodcock 2003).

5.2. Classification Model Evaluation by Vegetation Class

Deciduous had the consistently highest accuracies of any vegetation class. The lowest reported accuracy throughout all scenes was 89.9% and the highest was 98.4%. Possible reasons for such

high accuracy for this class could be that this class occurs in large, relatively homogenous stretches throughout the scene, and this class had additional training data in the form of the digitized polygons. For the deciduous class the lower accuracies were producer's accuracy and the highest were user's accuracy. This means the error of omission is higher than the error of commission and the classifier is leaving out or misclassifying the reference deciduous ground truth points (Congalton, 1991), often confusing deciduous for mixed forest, evergreen, and then shrub/scrub.

Evergreen forest also performed very well throughout all the scenes with the lowest accuracy reported at 81.6% and the highest at 97.7%. Like the deciduous class, this class also occurred in large swatches of area throughout the scene, and had additional training polygons, resulting in the high accuracies. Evergreen was the dominant vegetation class throughout all the maps, although the percentage of pixels varied throughout the years. In the 1985 map, evergreen only accounted for 27.2% of the pixels. The amount of shrub was very high, 21.7%, in the 1985 map in comparison to other years. The northwest scene specifically was classified as almost entirely shrub and emergent herbaceous wetlands, where in the other years a significant amount of those pixels were classified as evergreen. This is believed to be an error and is further discussed in section 5.3. As with the deciduous class, the user's accuracy was higher than the producer's accuracy and was often confused with woody wetlands, mixed forest, and deciduous forest.

Mixed forest was one of the lower performing classes, having a wide range of accuracies between 53.5-90.0%. The user's accuracy accounts for the lower end of the values, ranging from 53.5-80.1%, with producer's accuracy ranging between 67.7-90.0%. Having a high producer's accuracy, but a low user's accuracy means the classifier is correctly classifying the training data as the correct class (in this case mixed forest), but it is also misclassifying other classes into the class, especially evergreen and deciduous (Congalton, 1991). This leaves us to believe that mixed forest is likely hard to differentiate spectrally from the other two forest classes as it was often misclassifying evergreen or deciduous training points as mixed forest.

The dwarf shrub class performed moderately throughout the maps, having wide ranges between 65.3-94.7%. User's accuracies were lower with range between 65.3-94.4% and producer's accuracies were higher with ranges between 76.2-94.7%. One cause of these ranges could be that most of the time, dwarf shrub is growing in areas where there is also barren land. When points of dwarf shrub are buffered, it is likely that some of these polygons overlapped into areas of barren land, confusing the spectral signature.

Shrub performed moderately throughout the years, with accuracies between 67.3-92.6%. Shrub was the second most widespread vegetation cover type in all the maps, accounting for 21.7%, 16.9%, 14.9%, and 16.0% of pixels for the 1985, 1995, 2005, and 2015 maps, respectively. As mentioned above, the percentage of pixels for the 1985 map are very high, mostly likely being an error introduced by the two late acquisition dates for two of the scenes.

Sedge and grassland were the two rarest classes of all the maps, only making up between 0.2-0.5% and 0.2-0.3% of pixels, respectively and had very little change to or from any of the other classes. Sedge and grassland also had some of the lowest accuracy rates. Sedge had wide ranges of accuracy from 39.5-91.3%. Sedge performed better in the northwest and southwest scenes where there were more training data. Sedge also had higher producer's accuracies than user's accuracies, consistently being confused with shrub and emergent herbaceous wetlands. Grassland had ranges of accuracies between 38.1-96.8%. Like sedge, grassland also had low user's accuracy and high producer's accuracy, consistently misclassifying shrub and emergent herbaceous wetlands into its class. Both sedge and grassland has very low numbers of training points, which could mean they are under sampled in the training data or just do not represent a large percentage of the study area. An increase in the number of training points tends to increase the accuracy (Rokach and Maimon, 2008). The low values and wide ranges of accuracies are most likely resulting from the fact that sedge and grassland do not populate large homogenous areas and are often found in association with other classes (Selkowitz and Stehman, 2011), and have a low number of training points within these classes.

Woody wetlands and emergent herbaceous performed moderately, having similar ranges for both user's and producer's accuracies from 64.9-93.7%, and 45.0-90.0%, respectively. These wide ranges of accuracies likely result from the fact that wetlands are notoriously hard to map using remote sensing data, as the spectral reflectance of wetlands not only contain the vegetation spectra, but are also combined with spectra from the soil, hydrology of the area, and the atmospheric vapor present in the environment (Adam et al., 2010; Lin, 2006; Zomer et al., 2009). Woody wetlands were most often misclassified as emergent herbaceous wetlands, evergreen forest, or shrub. Emergent herbaceous wetlands were most often classified as shrub, woody wetlands, or evergreen forest.

Barren land performed well with accuracies between 54.1-96.5% and was most often misclassified as dwarf shrub, shrub, and evergreen. As mentioned above, a likely cause for the wide ranges of accuracies is the buffered areas of dwarf shrub overlapping onto barren land and confusing the spectral signature. Barren land also had the fewest amount of training pixels, right behind sedge and grassland, even with the digitized polygons. Barren land experienced few changes throughout the decades and generally represented around 4% of pixels for each map.

Open water and ice/snow consistently had the highest accuracies, both user's and producer's at or above 98.3%, despite their scarcity in the scene. Open water was stable throughout all the maps, making up only around 1.7-2.0% of the pixels in each map. Ice/snow made up around 3% of pixels in each map, except the 1985 map that had a late acquisition date, which resulted in a much larger snowpack in the scene making up 7.2% of pixels. Neither class had significant change to or from any other class. Even though they contribute very few pixels to the overall map, their high accuracy rates result from their spectral signatures being very distinguishable from the vegetation (Selkowitz and Stehman, 2001).

5.3. Cross Tabulated Area Analysis

The cross tabulated area tables show the changes in vegetation in percent of area. Many classes experienced little to no change, such as emergent herbaceous wetlands, sedge, grassland, open water, and barren land. Changes in the ice/snow class correlate with the visual changes seen in the amount of snowpack for the images. The evergreen forest class has shown a steady decrease of the percentage of pixels declining from 41.3%, 39.7%, and 37.0% throughout 1995, 2005, and 2015, respectively. This trend may suggest a decrease in the growth and health of evergreen trees, which has been reported as a reaction to warming climate in the Arctic and Sub-arctic (Goetz et al., 2005; Beck et al., 2011; Verbyla, 2008; Soja et al., 2007). The cross tabulated area tables show evergreen pixels changing to two different classes, shrub and woody wetlands. From 1985-2015, the area of evergreen changing to shrub was 1.8%, 3.6%, and 3.3%. These areas where evergreen is transitioning to shrub could represent areas recovering from fires and could support the idea that deciduous shrub cover is increasing and is establishing quickly after disturbances (Viereck, 1979; Suarez et al., 1999; Lloyd, 2005; Xu et al., 2013). For the same time period, the percent area of evergreen changing to woody wetlands was 1.5%, 2.3%, and 4.7%. This increase in amount of area changing from evergreen to woody wetlands complements the fact that the percentage of woody wetland pixels have been steadily increasing from 6.9%, 8.9% and 10.7% from 1995 to 2015. This trend is in agreement with studies suggesting an increase in permafrost degradation is contributing to wetland distribution (Payette and Delwaide, 2004; Rowland et al., 2010; Smith et al., 2005).

As mentioned above, difficulties were encountered in mapping the northwest and northeast scenes in the 1985 map. For the 1985 map, the percentage of pixels for the evergreen class was relatively low at 27.2% compared to between 41.3-37.0% for all of the following years. The 1985 map also showed unusually high percentages of shrub at 27.1% compared to between 16.9-14.9% for the following years and emergent herbaceous wetlands at 13.7% compared to between 7.2-7.8% for the following years. This is believed to be an error. One possible reason could be that training data from future years, that has experienced successional changes, is overlaying

areas that have not experienced these changes yet, and the algorithm is confusing the spectral signature and what the training data is presenting. The belief that this section of the classified image is an error is further strengthened by the fact that (1) 7.5% area of shrub pixels changed to evergreen pixels between the years 1985-1995, and (2) when only considering the southwest and southeast scenes for the 1985 map, the percentage of area of evergreen pixels drops to 36.8%.

Throughout this study, ground truth points intersecting fire scars have been removed, as these areas are most likely to experience vegetation change from the fire disturbance. To investigate how much change is occurring outside the influence of fire disturbance, cross tabulated area charts were generated between the years of 1985-2015 (table 21) and 1995-2015 (table 22) with all fire scars masked. Looking at these tables, one can see that change is still happening in the areas outside of fire scars, but the amount of change is less significant. When looking at table 22, areas of evergreen are still changing to shrub, but the percentage of change through the 20-year difference is less than the change found between both the two 10-year periods. For example, the percentage of area changed from evergreen to shrub between 1995-2015 (20-year difference) is only 2.8%, less than the changes seen from 1995-2005 (3.6%), and 2005-2015 (3.3%). It could also be that other disturbances are the cause of some of these changes. Although forest fire is the major disturbance for the state of Alaska, the boreal forest throughout Alaska is also affected by insect infestation and plant disease, drought, and permafrost degradation. Bark beetle infestations cause widespread tree mortality, alter the structure of the forest, and in turn can lead to changes in forest composition that follow outbreak for several decades (Allen et al., 2006; Raffa et al., 2008). Drought has been shown to have a negative effect on the growth and health of coniferous species in the Alaskan boreal forest (Barber et al., 2000; Beck et al., 2011; Goetz et al., 2005; Verbyla, 2008). Permafrost influences soil temperature and moisture, subsurface hydrology, rooting zones, and nutrient cycling, all of which affect the productivity of vegetation. Permafrost degradation can convert terrestrial ecosystems to aquatic or wetland ecosystems throughout boreal forests on ice-rich permafrost (Jorgenson and Osterkamp, 2005; Jorgenson et al., 2001).

5.4. Comparative Analysis of Vegetation Classification Maps

The 1985 map had an overall weighted accuracy of 93.2%, followed by 88.4%, 93.3%, and 86.9% for the 1995, 2005, and 2015 maps, respectively. The 2015 map had the least number of training points available, as this map contained the most fire scars, and points from all fire scars were removed, resulting in the least accurate map. The 1995 map had the second least amount of training data, because many points needed to be removed due to the extent of the cloud cover. These accuracies found in this study are comparable or better than those found in the USGS NLCD 2001 Alaska mapping zone 70, which included all four scenes used in this study, resulting in an 81.8% accuracy value (this information is located within the metadata for the USGS NLCD 2001 map). This increase in accuracy most likely results from the increase in ground truth data in this study compared to the amount of ground truth data used in the USGS products, strengthening the idea that classification accuracy has a positive correlation with training data when using decision trees. It has to be kept in mind that the area from which the accuracy result is coming from for the USGS product is made up of several more paths and rows and is a much larger area.

6. CONCLUSION AND FUTURE IMPROVEMENTS

Within this study, four vegetation maps of a selected area within the boreal forest surrounding Fairbanks, Alaska have been generated using Landsat 4 and 5 TM and Landsat 8 OLI surface reflectance products at 30 meter spatial resolution using a decision tree classification. These maps include 9 vegetation classes, as well as barren land, open water, and ice/snow classes that are consistent with the classes identified in the 2001 USGS NLCD map of Alaska. This study has further demonstrated that it is possible to map the vegetation of the Alaskan boreal forest surrounding Fairbanks, Alaska with the combination of spectral and spatial resolution Landsat satellites provide.

These maps were created to the best of our ability to be comparable to the USGS NLCD products following the methodologies laid out in Homer et al. (2004) for the generation of the USGS NLCD 2001 map of Alaska. Certain challenges regarding the location of the study area were faced with the following adaptations to the methodology: reducing the number of Landsat scenes to just one for each path and row due to the scarcity of cloud-free images and the shortened length of seasons and buffering the ground truth data points to increase the amount of training data in each scene as well as introducing digitizing larger training polygons of certain classes. Overall weighted accuracies of 93.2%, 88.4%, 93.3%, and 86.9% were reached for the 1985, 1995, 2005, and 2015 maps, respectively, compared to 81.8% accuracy for the USGS product. Although these changes to the methodology were necessary, the four vegetation maps generated in this study are comparable or better than the first order of data quality using cross validation as the USGS NLCD 2001 product for Alaska, suggesting that the NLCD methodology for the boreal forest in interior Alaska will benefit from the presented refinements.

Trends found in this study may suggest the following changes to the boreal forest surrounding Fairbanks, Alaska: a decrease in the growth of evergreen forests, an expansion of shrubland, and an increase in wetland distribution, all of which have been reported as reactions to a warming climate in the Arctic and Sub-arctic (Heskel et al., 2013; Myers-Smith et al., 2011; Payette and

Delwaide, 2004; Rowland et al., 2010; Smith et al., 2005; Soja et al., 2007; Sturm et al., 2001; Tape et al., 2006).

Throughout this process, several suggestions for the future have been found. As mentioned above, completing a full radiometric correction, correcting for both topography and atmospheric effect, may enhance the final classification. In this case, a DEM would not be needed. Although, the greatest chances to improve this process would be to personally collect a set of training data. For the case of Alaska, researchers face the following challenges that often prevent this: the expansiveness of the state, lack of road systems that make most of the state inaccessible, short summer season in which to collect vegetation data, and the inability to collect vegetation data in the winter due to the extreme climate. Alaska also lacks coverage of ancillary data, such as accurate inventories of wetlands, soils, and other environmental characteristics. The same challenges apply to collecting ancillary data and this restricts the buildup of statewide databases of ecological inventories like some states have. For these reasons, incorporating different types of remote sensing data to supplement the Landsat imagery might improve the generating of vegetation maps. High resolution imagery, such as from IKONOS (4 m spatial resolution), SPOT (2.5 m spatial resolution), or QuickBird (2.6 m spatial resolution) would assist in increasing the amount of training data (digitized polygons) for classes by aiding visual interpretation. Mapping a large area using only high resolution satellite imagery might be difficult due to the smaller scene dimension (IKONOS – 11 x 11 km, SPOT – 60 x 60 km, and Quickbird 16.5 x 16.5 km, compared to Landsat 4-5, 8 – 185 x 185 km scene dimensions) but would be useful to aid in areas of confusion or difficulty. Hyperspectral imagery such as from AVIRIS or Hyperion would also be useful in identifying especially complex vegetation classes, such as wetlands (Adam, et al., 2010), or classes that often overlap or are located in association with one another, such as barren land and dwarf shrub. Challenges also come with hyperspectral imaging. The amount of information that needs to be stored and processed (for example, 1 Hyperion scene is over 1 GB of data) can be difficult, and the fact that the swaths are small means more pieces to mosaic and opportunities for clouds, phenology, etc. become an increasing problem. Using this data for specific areas instead of trying to cover an entire large area of study would be more ideal. Information on how high resolution

imagery and hyperspectral imagery has been used in mapping vegetation can be found in the review paper by Xie et al. (2008). A third type of remote sensing data that would be helpful is light detection and ranging (LiDAR). LiDAR sensors measure the 3-dimensional distribution of plant canopies and the topography underneath the canopies, and although they have no spectral component they can make highly accurate estimations of vegetation height and canopy structure (Genc et al., 2004). Knowing the height of vegetation would aid in distinguishing areas of shrub and dwarf shrub and could also help distinguish between woody wetlands and emergent herbaceous wetlands (Genc et al., 2004; Greaves et al., 2016; Lin and Liquan, 2006; Luo et al., 2015). As mentioned above, Alaska is unique in its large size and remoteness in combination with its abnormal climate and amount of cloud cover; for these reasons it would be beneficial to incorporate more multisensor and multiresolution data to improve the classification methodology.

References

Adam, E., Mutanga, O. and Rugege, D., 2010. Multispectral and hyperspectral remote sensing for identification and mapping of wetland vegetation: a review. *Wetlands Ecology and Management*, *18*(3), pp. 281-296.

Allen, J.L., Wesser, S., Markon, C.J. and Winterberger, K.C., 2006. Stand and landscape level effects of a major outbreak of spruce beetles on forest vegetation in the Copper River Basin, Alaska. *Forest Ecology and Management*, *227*(3), pp. 257-266.

Anderson, J.R., 1976. *A land use and land cover classification system for use with remote sensor data* (Vol. 964). US Government Printing Office.

Barber, V.A., Juday, G.P. and Finney, B.P., 2000. Reduced growth of Alaskan white spruce in the twentieth century from temperature-induced drought stress. *Nature*, *405*(6787), p.668.

Basham May, A.M., Pinder III, J.E. and Kroh, G.C., 1997. A comparison of Landsat Thematic Mapper and SPOT multi-spectral imagery for the classification of shrub and meadow vegetation in northern California, USA. *International Journal of Remote Sensing*, *18*(18), pp. 3719-3728.

Beck, P.S., Goetz, S.J., Mack, M.C., Alexander, H.D., Jin, Y., Randerson, J.T. and Loranty, M.M., 2011. The impacts and implications of an intensifying fire regime on Alaskan boreal forest composition and albedo. *Global Change Biology*, *17*(9), pp. 2853-2866.

Bhatt, U.S., Walker, D.A., Raynolds, M.K., Comiso, J.C., Epstein, H.E., Jia, G.S., Gens, R., Pinzon, J.E., Tucker, C.J., Tweedie, C.E., Webber, P.J., 2010. Circumpolar Arctic tundra vegetation change ss linked to sea ice decline. *Earth Interact,* 14, pp. 1-20.

Boggs, K., Boucher, T.V., Kuo, T.T., Fehringer, D. and Guyer, S., 2012. Vegetation map and classification: Northern, western and interior Alaska. *Anchorage: Alaska Natural Heritage Program, University of Alaska*.

Chapin, F.S., McGuire, A.D., Randerson, J., Pielke, R., Baldocchi, D., Hobbie, S.E., Roulet, N., Eugster, W., Kasischke, E., Rastetter, E.B. and Zimov, S.A., 2000. Arctic and boreal ecosystems

of western North America as components of the climate system. *Global Change Biology*, *6*(S1), pp. 211-223.

Coppin, P., Lambin, E., Jonckheere, I. and Muys, B., 2002. Digital change detection methods in natural ecosystem monitoring: A review. *Analysis of multi-temporal remote sensing images*, pp. 3-36.

Cingolani, A.M., Renison, D., Zak, M.R. and Cabido, M.R., 2004. Mapping vegetation in a heterogeneous mountain rangeland using Landsat data: an alternative method to define and classify land-cover units. *Remote Sensing of Environment*, *92*(1), pp. 84-97.

Comer P, Faber-Langendoen D, Evans R, Gawler S, Josse C, Kittel G, Menard S, Pyne M, Reid M, Schulz K, Snow K, Teague J., 2003. Ecological systems of the United States: a working classification of US terrestrial systems. *NatureServe*, Arlington, VA. Available at http://www. natureserve.org/library/usEcologicalsystems.pdf

Congalton, R.G., 1991. A review of assessing the accuracy of classifications of remotely sensed data. *Remote Sensing of Environment*, *37*(1), pp. 35-46.

Dymond, C.C., Mladenoff, D.J. and Radeloff, V.C., 2002. Phenological differences in Tasseled Cap indices improve deciduous forest classification. *Remote Sensing of Environment*, 80(3), pp. 460-472.

Freund, Y. and Schapire, R.E., 1996, Experiments with a new boosting algorithm. In *International Conference on Machine Learning*, 96, pp. 48-156.

Friedl, M.A. and Brodley, C.E., 1997. Decision tree classification of land cover from remotely sensed data. *Remote Sensing of Environment*, *61*(3), pp. 399-409.

Foga, S., Scaramuzza, P.L., Guo, S., Zhu, Z., Dilley, R.D., Beckmann, T., Schmidt, G.L., Dwyer, J.L., Hughes, M.J. and Laue, B., 2017. Cloud detection algorithm comparison and validation for operational Landsat data products. *Remote sensing of environment*, *194*, pp. 379-390.

Genç, L., Dewitt, B. and Smith, S., 2004. Determination of wetland vegetation height with LIDAR. *Turkish Journal of Agriculture and Forestry*, 28(1), pp. 63-71.

Gens, R. and Cristóbal, J. 2016. Remote Sensing Data Normalization. In Remote Sensing Handbook Volume I. Remotely sensed data characterization, classification, and accuracies. CRC Press. Taylor and Francis. ISBN: 13: 978-1-4822-1787-2.

Gesch, D., Oimoen, M., Greenlee, S., Nelson, C., Steuck, M. and Tyler, D., 2002. The national elevation dataset. *Photogrammetric Engineering and Remote Sensing*, *68*(1), pp. 5-32.

Goetz, S.J., Bunn, A.G., Fiske, G.J. and Houghton, R.A., 2005. Satellite-observed photosynthetic trends across boreal North America associated with climate and fire disturbance. *Proceedings of the National Academy of Sciences of the United States of America*, *102*(38), pp. 13521-13525.

Greaves, H.E., Vierling, L.A., Eitel, J.U., Boelman, N.T., Magney, T.S., Prager, C.M. and Griffin, K.L., 2016. High-resolution mapping of aboveground shrub biomass in Arctic tundra using airborne lidar and imagery. *Remote sensing of environment*, 184, pp. 361-373.

Grossman, D.H., Faber-Langendoen, D., Weakley, A.S., Anderson, M., Bourgeron, P., Crawford, R., Goodin, K., Landaal, S., Metzler, K., Patterson, K.D. and Pyne, M., 1998. International classification of ecological communities: terrestrial vegetation of the United States. *The Nature Conservancy, Arlington, Virginia*.

Harvey, K.R. and Hill, G.J.E., 2001. Vegetation mapping of a tropical freshwater swamp in the Northern Territory, Australia: a comparison of aerial photography, Landsat TM and SPOT satellite imagery. *International Journal of Remote Sensing*, *22*(15), pp. 2911-2925.

Heskel, M., Greaves, H., Kornfeld, A., Gough, L., Atkin, O. K., Turnbull, M. H., Shaver, and G., Griffin, K. L., 2013. Differential physiological responses to environmental change promote woody shrub expansion. *Ecology and Evolution*, 3(5), pp. 1149–1162.

Hinzman, L.D., Viereck, L.A., Adams, P.C., Romanovsky, V.E. and Yoshikawa, K., 2006. Climate and permafrost dynamics of the Alaskan boreal forest. *Alaska's Changing Boreal Forest*, pp. 39-61.

Hobbs, R.J., 1990. Remote sensing of spatial and temporal dynamics of vegetation. In Remote sensing of biosphere functioning, pp. 203-219. Springer, New York, NY.

Hollingsworth, J. 2010. *Bonanza Creek Experimental Forest GIS Data: Research Area Boundary (NAD83)*, Bonanza Creek LTER - University of Alaska Fairbanks.

Homer, C.G., Dewitz, J.A., Yang, L., Jin, S., Danielson, P., Xian, G., Coulston, J., Herold, N.D., Wickham, J.D., and Megown, K., 2015. Completion of the 2011 National Land Cover Database for the conterminous United States-Representing a decade of land cover change information. *Photogrammetric Engineering and Remote Sensing*, 81(5), pp. 345-354.

Homer, C., Dewitz, J., Fry, J., Coan, M., Hossain, N., Larson, C., Herold, N., McKerrow, A., VanDriel, J.N. and Wickham, J., 2007. Completion of the 2001 national land cover database for the counterminous United States. *Photogrammetric engineering and remote sensing*, *73*(4), p.337.

Homer, C., Huang, C., Yang, L., Wylie, B. and Coan, M., 2004. Development of a 2001 national land-cover database for the United States. *Photogrammetric Engineering & Remote Sensing*, *70*(7), pp. 829-840.

Jia, G.J., Epstein, H.E. and Walker, D.A., 2003. Greening of Arctic Alaska, 1981–2001. *Geophysical Research Letters*, 30(20), pp. 2067.

Johnstone J.F., Hollingsworth T.N., Chapin III F.S., and Mack M.C., 2010a. Changes in fire regime break the legacy lock on successional trajectories in Alaskan boreal forest. *Global Change Biology*, 16(4), pp. 1281-1295.

Johnstone, J.F., Chapin, F.S., Hollingsworth, T.N., Mack, M.C., Romanovsky, V. and Turetsky, M., 2010b. Fire, climate change, and forest resilience in interior Alaska. *Canadian Journal of Forest Research*, *40*(7), pp. 1302-1312.

Jorgenson, M.T. and Osterkamp, T.E., 2005. Response of boreal ecosystems to varying modes of permafrost degradation. *Canadian Journal of Forest Research*, *35*(9), pp. 2100-2111.

Jorgenson, M.T., Racine, C.H., Walters, J.C. and Osterkamp, T.E., 2001. Permafrost degradation and ecological changes associated with a warming climate in Central Alaska. *Climatic Change*, *48*(4), pp. 551-579.

Kaufman, Y.J., Wald, A.E., Remer, L.A., Gao, B.C., Li, R.R. and Flynn, L., 1997. The MODIS 2.1-/spl mu/m channel-correlation with visible reflectance for use in remote sensing of aerosol. *IEEE Transactions on Geoscience and Remote Sensing*, 35(5), pp. 1286-1298.

Kasischke, E.S. and Stocks, B.J. eds., 2012. Fire, climate change, and carbon cycling in the boreal forest. *Springer Science & Business Media, 138.*

Kasischke, E.S. and Turetsky, M.R., 2006. Recent changes in the fire regime across the North American boreal region—spatial and temporal patterns of burning across Canada and Alaska. *Geophysical Research Letters*, *33*(9).

Kim, Y., Hatsushika, H., Muskett, R.R. and Yamazaki, K., 2005. Possible effect of boreal wildfire soot on Arctic sea ice and Alaska glaciers. *Atmospheric Environment*, *39*(19), pp. 3513-3520.

Kussul, N., Skakun, S., Shelestov, A., Lavreniuk, M., Yailymov, B. and Kussul, O., 2015. Regional scale crop mapping using multi-temporal satellite imagery. *The International Archives of Photogrammetry, Remote Sensing and Spatial Information Sciences*, *40*(7), p. 45.

LANDFIRE, 2012a, Existing Vegetation Type Layer, LANDFIRE 1.0.0, US Department of Interior, US Geological Survey. Accessed at https://www.landfire.gov/geoareasmaps/2012/AK_EVT_c12.pdf

LANDFIRE, 2012b, Vegetation Disturbance Layer, LANDFIRE 1.0.0, US Department of Interior, US Geological Survey. Accessed at https://www.landfire.gov/lf_applications.php#maps

LANDFIRE, 2001, LANDFIRE Reference Database, LANDFIRE 1.0.0, US Department of Interior, US Geological Survey. Accessed at https://www.landfire.gov/lfrdb_data.php

Lin Y and Liquan Z, 2006. Identification of the spectral characteristics of submerged plant Vallisneria spiralis. *Acta Ecologica Sinica,* 26, pp. 1005–1011

Liu, Y., Goodrick, S. and Heilman, W., 2014. Wildland fire emissions, carbon, and climate: Wildfire–climate interactions. *Forest Ecology and Management*, *317*, pp. 80-96.

Lloyd, A.H., 2005. Ecological histories from Alaskan tree lines provide insight into future change. *Ecology*, 86, pp. 1687-1695.

Luo, S., Wang, C., Pan, F., Xi, X., Li, G., Nie, S. and Xia, S., 2015. Estimation of wetland vegetation height and leaf area index using airborne laser scanning data. *Ecological Indicators*, 48, pp. 550-559.

Masek, J.G., Vermote, E.F., Saleous, N.E., Wolfe, R., Hall, F.G., Huemmrich, K.F., Gao, F., Kutler, J. and Lim, T.K., 2006. A Landsat surface reflectance dataset for North America, 1990-2000. *IEEE Geoscience and Remote Sensing Letters*, *3*(1), pp. 68-72.

McGuire, A.D., Anderson, L.G., Christensen, T.R., Dallimore, S., Guo, L., Hayes, D.J., Heimann, M., Lorenson, T.D., Macdonald, R.W. and Roulet, N., 2009. Sensitivity of the carbon cycle in the Arctic to climate change. *Ecological Monographs*, *79*(4), pp. 523-555.

Myers-Smith, I.H., Forbes, B.C., Wilmking, M., Hallinger, M., Lantz, T., Blok, D., Tape, K.D., Macias-Fauria, M., Sass-Klaassen, U., Lévesque, E. and Boudreau, S., 2011. Shrub expansion in tundra ecosystems: dynamics, impacts and research priorities. *Environmental Research Letters*, *6*(4), p. 045509.

Ott, L.A.V.R.A., Mann, P.C.A.D. and Van Cleve, K., 2006. Successional processes in the Alaskan boreal forest. *Alaska's Changing Boreal Forest*, p. 100.

Pal, M. and Mather, P.M., 2003. An assessment of the effectiveness of decision tree methods for land cover classification. *Remote Sensing of Environment*, *86*(4), pp. 554-565.

Payette, S. and Delwaide, A., 2004. Dynamics of subarctic wetland forests over the past 1500 years. *Ecological Monographs*, *74*(3), pp. 373-391.

Pons, X., Pesquer, L., Cristóbal, J. and González-Guerrero, O., 2014. Automatic and improved radiometric correction of Landsat imagery using reference values from MODIS surface reflectance images. *International Journal of Applied Earth Observation and Geoinformation*, *33*, pp. 243-254.

Proy, C., Tanre, D. and Deschamps, P.Y., 1989. Evaluation of topographic effects in remotely sensed data. *Remote Sensing of Environment*, 30(1), pp. 21-32.

Quinlan, J.R., 1993. C4. 5: Programming for machine learning. *Morgan Kauffmann*, *38*, p. 48.

Quinlan, J.R., 1996. Bagging, boosting and C4.5. *American Association for Artıficial Intelligence,* pp. 725-730.

Raffa, K.F., Aukema, B.H., Bentz, B.J., Carroll, A.L., Hicke, J.A., Turner, M.G. and Romme, W.H., 2008. Cross-scale drivers of natural disturbances prone to anthropogenic amplification: the dynamics of bark beetle eruptions. *AIBS Bulletin*, *58*(6), pp. 501-517.

Riaño, D., Chuvieco, E., Salas, J. and Aguado, I., 2003. Assessment of different topographic corrections in Landsat-TM data for mapping vegetation types (2003). *IEEE Transactions on Geoscience and Remote Sensing*, 41(5), pp. 1056-1061.

Rieger, S., Dement, JA., and Sanders, D., 1963. *Soil survey, Fairbanks area, Alaska* (No. 1723). US Department of Agriculture, Soil Conservation Service.

Rokach, L. and Maimon, O.Z., 2008. Data mining with decision trees: theory and applications. *Series in Machine Perception and Artıficial Intelligence*, 69.

Rollins, M.G., 2009. LANDFIRE: a nationally consistent vegetation, wildland fire, and fuel assessment. *International Journal of Wildland Fire*, *18*(3), pp. 235-249.

Rowland, J.C., Jones, C.E., Altmann, G., Bryan, R., Crosby, B.T., Hinzman, L.D., Kane, D.L., Lawrence, D.M., Mancino, A., Marsh, P. and McNamara, J.P., 2010. Arctic landscapes in transition: responses to thawing permafrost. *Eos, Transactions American Geophysical Union*, *91*(26), pp. 229-230.

Schroeder, T.A., Cohen, W.B., Song, C., Canty, M.J. and Yang, Z., 2006. Radiometric correction of multi-temporal Landsat data for characterization of early successional forest patterns in western Oregon. *Remote Sensing of Environment*, 103(1), pp. 16-26.

Selkowitz, D.J. and Stehman, S.V., 2011. Thematic accuracy of the National Land Cover Database (NLCD) 2001 land cover for Alaska. *Remote Sensing of Environment*, 115(6), pp. 1401-1407.

Serreze, M.C. and Barry, R.G., 2011. Processes and impacts of Arctic amplification: A research synthesis. *Global and planetary change*, *77*(1-2), pp. 85-96.

Serreze, M.C., Walsh, J.E., Chapin, F.S., Osterkamp, T., Dyurgerov, M., Romanovsky, V., Oechel, W.C., Morison, J., Zhang, T. and Barry, R.G., 2000. Observational evidence of recent change in the northern high-latitude environment. *Climatic Change*, *46*(1-2), pp. 159-207.

Sexton, J.O., Urban, D.L., Donohue, M.J. and Song, C., 2013. Long-term land cover dynamics by multi-temporal classification across the Landsat-5 record. *Remote Sensing of Environment*, 128, pp. 246-258.

Smith, L.C., Sheng, Y., MacDonald, G.M. and Hinzman, L.D., 2005. Disappearing arctic lakes. *Science*, *308*(5727), pp. 1429-1429.

Son, N.T., Chen, C.F., Chen, C.R., Duc, H.N. and Chang, L.Y., 2013. A phenology-based classification of time-series MODIS data for rice crop monitoring in Mekong Delta, Vietnam. *Remote Sensing*, *6*(1), pp. 135-156.

Soja, A.J., Tchebakova, N.M., French, N.H., Flannigan, M.D., Shugart, H.H., Stocks, B.J., Sukhinin, A.I., Parfenova, E.I., Chapin, F.S. and Stackhouse, P.W., 2007. Climate-induced boreal forest change: predictions versus current observations. *Global and Planetary Change*, *56*(3), pp. 274-296.

Song, C. and Woodcock, C.E., 2003. Monitoring forest succession with multitemporal Landsat images: Factors of uncertainty. *IEEE Transactions on Geoscience and Remote Sensing*, 41(11), pp. 2557-2567.

Song, C., Woodcock, C.E., Seto, K.C., Lenney, M.P. and Macomber, S.A., 2001. Classification and change detection using Landsat TM data: when and how to correct atmospheric effects? *Remote Sensing of Environment*, 75(2), pp. 230-244.

Song, Y.Y. and Ying, L.U., 2015. Decision tree methods: applications for classification and prediction. *Shanghai Archives of Psychiatry*, *27*(2), p. 130.

Sturm, M., Racine, C. and Tape, K., 2001. Climate change: increasing shrub abundance in the Arctic. *Nature*, *411*(6837), p. 546.

Suarez, F., Binkley, D., Kaye, M.W. and Stottlemyer, R., 1999. Expansion of forest stands into tundra in the Noatak National Preserve, northwest Alaska. *Ecoscience*, *6*(3), pp. 465-470.

Tape, K.D., Sturm, M. and Racine, C., 2006. The evidence for shrub expansion in northern Alaska and the Pan-Arctic. *Global Change Biology*, *12*(4), pp.686-702.

U.S. Geological Survey, 2018. Surface Reflectance Product Guide. Accessed at https://landsat.usgs.gov/sites/default/files/documents/ledaps_product_guide.pdf

Ustin, S.L. and Xiao, Q.F., 2001. Mapping successional boreal forests in interior central Alaska. *International Journal of Remote Sensing*, *22*(9), pp. 1779-1797.

van Cleve, K., Dyrness, C.T., Viereck, L.A., Fox, J., Chapin III, F.S. and Oechel, W., 1983. Taiga ecosystems in interior Alaska. *Bioscience*, *33*(1), pp. 39-44.

Verbyla, D., 2008. The greening and browning of Alaska based on 1982–2003 satellite data. *Global Ecology and Biogeography*, *17*(4), pp. 547-555.

Vermote, E.F., Tanré, D., Deuze, J.L., Herman, M. and Morcette, J.J., 1997. Second simulation of the satellite signal in the solar spectrum, 6S: An overview. *IEEE Transactions on Geoscience and Remote Sensing*, 35(3), pp. 675-686.

Viereck, L.A., Dyrness, C.T., Batten, A.R. and Wenzlick, K.J., 1992. The Alaska vegetation classification: USDA Forest Service General Technical Report PNW-GTR-286. *Pacific northwest Research Station, Portland, Oregon, USA*.

Viereck, L.A., 1979. Characteristics of treeline plant communities in Alaska. *Ecography*, *2*(4), pp. 228-238.

Walsh, J.E., 2014. Intensified warming of the Arctic: Causes and impacts on middle latitudes. *Global and Planetary Change*, *117*, pp. 52-63.

Wolter, P.T., Mladenoff, D.J., Host, G.E. and Crow, T.R., 1995. Using multi-temporal Landsat imagery. *Photogrammetric Engineering & Remote Sensing*, *61*(9), pp. 1129-1143.

Xie, Y., Sha, Z. and Yu, M., 2008. Remote sensing imagery in vegetation mapping: a review. *Journal of Plant Ecology*, *1*(1), pp. 9-23.

Xu, L., Myneni, R.B., Chapin Iii, F.S., Callaghan, T.V., Pinzon, J.E., Tucker, C.J., Zhu, Z., Bi, J., Ciais, P., Tømmervik, H. and Euskirchen, E.S., 2013. Temperature and vegetation seasonality diminishment over northern lands. *Nature Climate Change*, *3*(6), p.581.

Yu, L., Holden, E.J., Dentith, M.C. and Zhang, H., 2012. Towards the automatic selection of optimal seam line locations when merging optical remote-sensing images. *International Journal of Remote Sensing*, *33*(4), pp. 1000-1014.

Zhao, F., Huang, C. and Zhu, Z., 2015. Use of vegetation change tracker and support vector machine to map disturbance types in greater Yellowstone ecosystems in a 1984–2010 Landsat time series. *IEEE Geoscience and Remote Sensing Letters*, *12*(8), pp. 1650-1654.

Zhu, Z., Wang, S. and Woodcock, C.E., 2015. Improvement and expansion of the Fmask algorithm: Cloud, cloud shadow, and snow detection for Landsats 4–7, 8, and Sentinel 2 images. *Remote Sensing of Environment*, *159*, pp. 269-277.

Zhu, Z. and Woodcock, C.E., 2012. Object-based cloud and cloud shadow detection in Landsat imagery. *Remote Sensing of Environment*, *118*, pp. 83-94.

Zhu, Z., Vogelmann, J., Ohlen, D., Kost, J., Chen, X., Tolk, B. and Rollins, M., 2006. Mapping existing vegetation composition and structure for the LANDFIRE prototype project. *The LANDFIRE Prototype Project: nationally consistent and locally relevant geospatial data for wildland fire management. USDA Forest Service General Technical Report RMRS-GTR-175, Fort Collins, Colorado: Rocky Mountain Research Station, USA*, pp. 197-215.

Zomer, R.J., Trabucco, A. and Ustin, S.L., 2009. Building spectral libraries for wetlands land cover classification and hyperspectral remote sensing. *Journal of Environmental Management*, *90*(7), pp. 2170-2177.